

Review

Gold and Silver Nanoparticle-Based Colorimetric Sensors: New Trends and Applications

Giancarla Alberti ^{1,*}, Camilla Zanoni ¹, Lisa Rita Magnaghi ^{1,2} and Raffaella Biesuz ^{1,2}

¹ Department of Chemistry, University of Pavia, Via Taramelli 12, 27100 Pavia, Italy; camilla.zanoni01@universitadipavia.it (C.Z.); lisarita.magnaghi01@universitadipavia.it (L.R.M.); raffaella.biesuz@unipv.it (R.B.)

² Unità di Ricerca di Pavia, INSTM, Via G. Giusti 9, 50121 Firenze, Italy

* Correspondence: galberti@unipv.it

Abstract: Gold and Silver nanoparticles (AuNPs and AgNPs) are perfect platforms for developing sensing colorimetric devices thanks to their high surface to volume ratio and distinctive optical properties, particularly sensitive to changes in the surrounding environment. These characteristics ensure high sensitivity in colorimetric devices. Au and Ag nanoparticles can be capped with suitable molecules that can act as specific analyte receptors, so highly selective sensors can be obtained. This review aims to highlight the principal strategies developed during the last decade concerning the preparation of Au and Ag nanoparticle-based colorimetric sensors, with particular attention to environmental and health monitoring applications.

Keywords: gold nanoparticles; silver nanoparticles; colorimetric devices; nanoparticle-based sensors



Citation: Alberti, G.; Zanoni, C.; Magnaghi, L.R.; Biesuz, R. Gold and Silver Nanoparticle-Based Colorimetric Sensors: New Trends and Applications. *Chemosensors* **2021**, *9*, 305. <https://doi.org/10.3390/chemosensors9110305>

Academic Editor: Zhuangqiang Gao

Received: 14 September 2021

Accepted: 24 October 2021

Published: 26 October 2021

Publisher's Note: MDPI stays neutral with regard to jurisdictional claims in published maps and institutional affiliations.



Copyright: © 2021 by the authors. Licensee MDPI, Basel, Switzerland. This article is an open access article distributed under the terms and conditions of the Creative Commons Attribution (CC BY) license (<https://creativecommons.org/licenses/by/4.0/>).

1. Introduction

Colorimetric methods draw attention due to their simplicity and low cost. Detection with these sensors is generally obtained merely by viewing with the naked eye the color changes, so no sophisticated or expensive additional devices are needed. Moreover, they can be used in field analysis and point-of-care testing [1]. Rapid and cost-effective colorimetric devices have demonstrated their good performance in biosensing, environmental monitoring and medical diagnosis. The development of these sensors has rapidly grown in recent years; this trend shows the deep interest of the scientific community in this field. The challenge in developing new colorimetric sensors with a simple naked-eye detection of the color changes induced by the analyte. For this purpose, several chromogenic substrates and color labels have been explored, particularly those with high selectivity, sensitivity, low cost and suitable for practical applications. Among them, dye-based and nanoparticles-based sensors have been widely studied [2,3].

Traditionally, dye-based colorimetric devices have attracted great attention thanks to their low cost, high stability, and usage for several applications, such as chemical and biochemical sensing, medical diagnosis and environmental analysis [1]. The functional principle of these colorimetric sensors depends on the color changes induced or mediated by an analyte after its reaction with the dye. Unfortunately, these methods are not very sensitive since the generally low extinction coefficients of the dyes and the scarce accuracy in perceiving small color variations by the naked eye. Moreover, it is often difficult to determine individual components of a mixture without employing chemometric methods [4].

Recently, great attention was paid to nanoparticle-based sensors due to the exceptional properties of nanomaterials, such as biocompatibility, conductivity and catalytic activity [5–7]. With nanomaterials the problems associated with traditional organic dye-based colorimetric devices can be overcome. In recent years, the use of nanomaterial-based

colorimetric sensors that can detect simply by the naked eye ultralow concentrations of target analytes has been widely studied [8,9].

Noble metal nanoparticles, provided with distinctive physicochemical and optical properties, display higher extinction coefficients than dyes, allowing one to sense target analytes by color changes detectable by the naked eye [10]. In addition, their unique localized surface plasmon resonance (LSPR) properties, associated with their characteristic colors, dispersion and aggregation status, make them ideal for sensitive colorimetric recognition of several chemical and biological analytes [11].

In the past decades, huge progress has been made in developing metal nanoparticle-based colorimetric devices which sensing mechanism is based on interparticle distance-dependent principles [12,13]. In these sensors, the nanoparticles' aggregation and dispersion grade variation, induced by the analyte, changes the interparticle plasmon coupling properties detectable by LSPR spectral shifts and the evident solution color changes [1]. From the first colorimetric device proposed by Mirkin et al. [14], several LSPR-based colorimetric sensors were developed for different analytes, such as macromolecules [15], living cells [16] and metal ions [17].

Unfortunately, this kind of sensor presents some disadvantages; for example, the colloidal nanoparticles' auto-aggregation leads to false positive or false negative results and lower selectivity in some analyses. Moreover, the lack of cheap methods that could improve the performance of naked-eye-based sensors is another crucial point [1].

The actual challenge is the growth of economic and trusted nanoparticle-based colorimetric sensors with great selectivity and sensitivity. The recent literature has reported new strategies for developing "non-aggregation" nanoparticle-based colorimetric sensors that rely on LSPR and will be potentially useful for detecting many analytes [3,18]; they show good figures of merit if compared with the classical devices [19].

Moreover, if compared with dye-based devices, metal nanoparticle-based sensors possess higher extinction coefficients, higher sensitivity, and better performances in colorimetric analyses [1].

Several reviews have been recently published; most of them have reported a description of a single class of metal nanoparticles or a particular field of application. Here we decide to summarize and review in depth both gold and silver nanoparticle-based colorimetric sensors describing the most innovative and newly developed devices. An in-depth discussion on the synthetic strategies and performances for all noble metals' nanoparticle-based sensors is outside the scope of the present review.

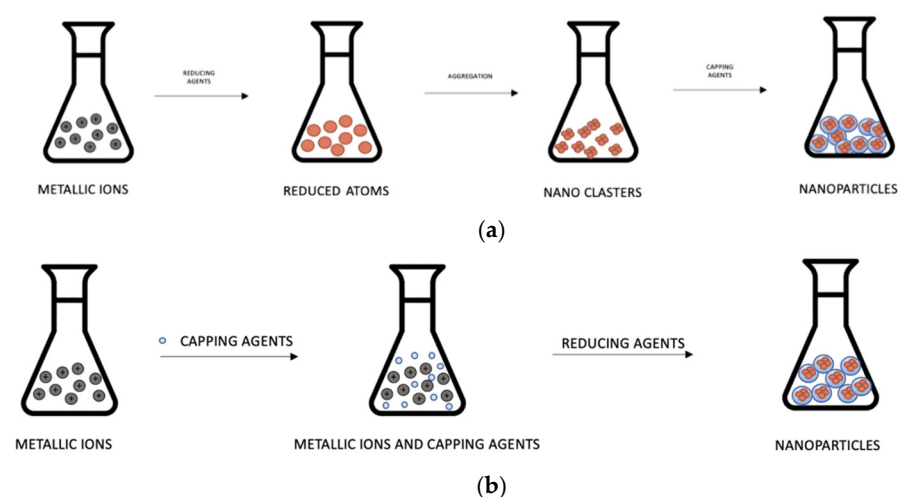
Hereafter, we present an overview of the application of Ag and Au nanoparticles for colorimetric sensors. The review is structured in six sections. The first is a general introduction; the second summarizes the different Au and Ag nanoparticles' synthesis strategies, functionalization, and properties. The third and fourth sections are respectively dedicated to the description of Ag and Au-NPs-based colorimetric sensors and some examples of their applications. The fifth section is dedicated to applications of Ag/Au bimetallic NPs. Finally, the last part highlights the progress and future perspectives of these nanomaterial-based devices.

2. AgNPs and AuNPs: Synthesis and Properties

IUPAC defines nanoparticles as "particles of any shape with dimensions in the 10^{-9} and 10^{-7} m range" [20]. Nowadays, nanoparticles (NP) are used in different fields such as textiles, cosmetics, pharmaceuticals, engineering, biology, and medicine. NP can be made of semiconductors, ceramics and polymers but is surprising that the properties of NPs have been utilized since ancient times [21]. One of the most famous examples is the *Licurgo cup*, dating from the IVth century, which presents different optical behaviors if illuminated from the inside or from the outside the cup: in reflected light, the cup assumes a yellow-green appearance, but in transmitted light, the color of the cup turns to red. These two effects are due to the presence of AgNP and AuNP inside the glass. There are many examples of objects containing metal NPs in history, such as the gold ruby glass used between the

IVth and the Vth century for mosaic decorations inside churches [21]. An ancient synthesis method for the preparation of metal nanoparticles was reported by Andreas Cassius of Leyden (1685) in the *De Auro* manuscript. Cassius described how to obtain “Purple of Cassius”: Au salts were dissolved in aqua regia and then precipitated with stannous and stannic chloride [21].

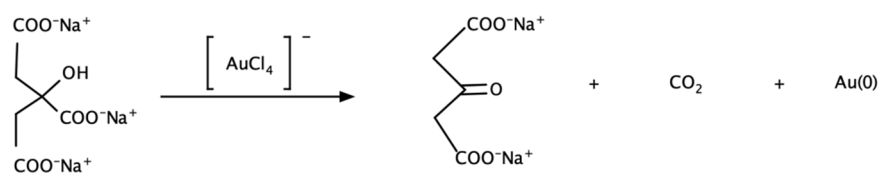
Two different strategies can be used in NP synthesis: bottom-up (Scheme 1a) or top-down approaches (Scheme 1b). In the top-down method, the starting material is bulk and must be reduced to smaller dimensions using destructive chemical-physical methods such as grinding, milling, or physical vapor deposition [22]. In the bottom-up methods, a soluble salt is dissolved in solution [23]. The choice of the solvent depends on the nature of the salt and the type of synthesis; they can be polar, apolar or water. Once the salt is dissolved, the metal center must be reduced to valence 0. The reducing agents might be gaseous hydrogen [24], hydride (NaBH_4) [24], organic reducing agents (citrate or ascorbic acid) [25,26], or biopolymers [27]. One of the biggest problems in NP synthesis is aggregation, which can be prevented thanks to the electrostatic charge on the particle's surface or steric stabilization [28].



Scheme 1. Scheme of NPs syntheses: (a) by the bottom-up method; (b) by the top-down method.

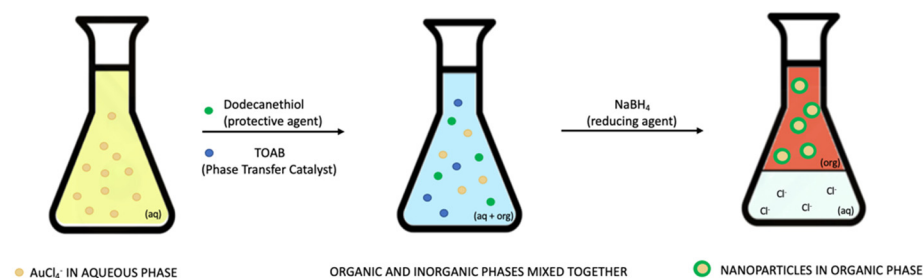
Moreover, stabilizers prevent uncontrolled growth due to the Ostwald ripening [29], maintaining under control the dimension of the particles [30], can induce anisotropic effects [31,32], and add new functions on the surface of the particle; this is a very important aspect for the creation of sensors. In some cases, the presence of new functions on the surface of the NP can induce the formation of dendrimers [33].

One of the most famous methods for AuNPs preparation is the 1951 Turkevich synthesis [34], in which HAuCl_4 is dissolved in deionized water and the solution is heated until it boils; then a solution of sodium citrate is added under stirring. The color of the solution will gradually change from yellow to grey, to purple, to deep purple, to finally dark red. First, the sodium citrate reacts as a reducing agent, then as a stabilizer because the negatively charged ions are adsorbed on the nanoparticles' surface, preventing aggregation. In this case, the surface of the nanoparticles is negatively charged. This method is very reproducible, and the nanoparticles have a low polydispersity. Scheme 2 shows the reduction mechanism of Au(III) by sodium citrate. The same method was applied to AgNPs synthesis, but it was necessary to use a stronger reducing agent such as NaBH_4 while sodium citrate was still used as a capping agent [35].



Scheme 2. Reduction mechanism of Au(III) by sodium citrate.

One of the problems of the synthesis in water is the trouble of obtaining NPs in the solid phase; indeed, upon removing the solvent, the particles tend to aggregate. A possible solution to this problem is a biphasic synthesis. The best-known method is the 1994 Brust-Schiffrin synthesis [36]. In this procedure, the metal salt is dissolved in water and carried into an organic phase (toluene) thanks to a phase transfer reagent (tetraoctylammonium bromide, TOAB), which will be reduced with a water solution of NaBH_4 in the presence of dodecanethiol as a protective agent. In this case, NPs are capped with thiol and might be precipitated, evaporating the solvent with ethanol in addition (see Scheme 3) [36].



Scheme 3. Scheme of phase-transfer NP synthesis.

Nanoparticles can have different shapes than spherical; for example, some widely used ones are Au nanostars [31], Ag nanoplates [37], Ag nanoprisms [38]. Figure 1 shows some SEM and TEM images of Ag and Au nanoparticles of different shapes.

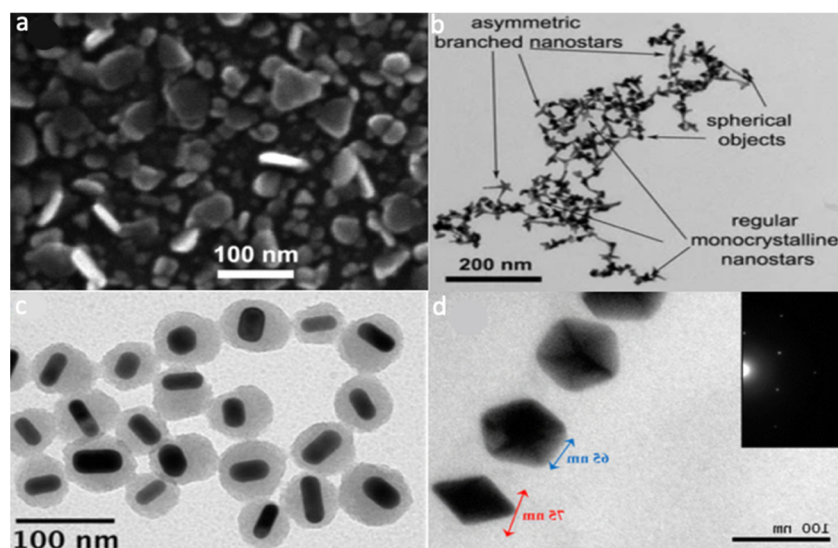


Figure 1. (a) SEM image of nano-plates Reprinted with permission from [39], copyright 2020, Elsevier B.V. (b) TEM image of nanostars. Reprinted with permission from [40] under Open Access Creative Common CC, license 4.0, to MDPI. (c) TEM image of nanorods. Reprinted with permission from [41], under Open Access Creative Common CC, license 4.0, to MDPI. (d) TEM image of pentagonal bipyramid nanoparticles. Reprinted with permission from [42], copyright 2016, American Chemical Society.

In order to obtain anisotropic shapes, the choice of the buffer and the capping agent is of paramount importance. For example, nanostars may be obtained using lauryl sulfobetaine (LSB) as a surfactant [31]; nanoplates need the presence of sodium citrate, which binds preferentially to a specific face of the crystal [37]; nanoprisms require the presence of NaBH_4 /citrate and H_2O_2 [38].

In recent years, the focus has moved to more sustainable chemistry; for this reason, it is interesting to know that some green procedures for the formation of NPs exist that exploit natural reducing agents. Vigneshwaran et al. described the one-pot synthesis of Ag nanoparticles in which starch acts both as a reducing and capping agent [43]. Nakhjavani et al. described how to obtain Ag NPs using the reducing and capping agents contained in tea leaves [4]. Daizy Philip instead described the method to obtain AuNPs using honey [44].

Nanoparticles are widely used thanks to their versatility and because they have totally different chemical-physical properties from their bulk material. For example, nanoparticles change their behavior upon varying the dimensions and the shape. Nanostars, nanoplates, nanoprisms, nanorods, beads, or spherical particles of the same metal will display different absorbance, reflectance, luminescence or fluorescence [45]. An interesting behavior of nanoparticles, absent in bulk material, is the localized plasma resonance (LSPR). This effect is generated when the incident radiation frequency is the same as the one needed to promote the electron in the conducting band. Experimentally it can be possible to observe the LSPR effect thanks to an absorption band with a high molar extinction coefficient [45].

In order to understand what the localized surface plasmon resonance (LSPR) effect is, we have to focus our attention on the interaction of light with a surface.

When light is totally reflected inside an optical fiber, the fiber's cladding may absorb the electric field of the radiation under certain conditions. The absorbed radiation is called *evanescent wave*, and the electric field is described as [46]:

$$E = E_0 \exp\left(-\frac{x}{dp}\right)$$

where E_0 is the electric field at the interface, x is the distance from the interface and dp is the penetration depth [46]:

$$dp = \frac{\lambda}{4\pi \sqrt{\sin^2 \theta - \left(\frac{n_2}{n_1}\right)^2}}$$

where λ is the excitation laser wavelength; θ is the angle between the incident ray and the normal of the surface; n_1 and n_2 are the refractive indexes of the core and the cladding, respectively [46].

If the cladding absorbs part of the radiation, the light intensity at the output of the optical fiber will be lower than at the input. This phenomenon is exploited to build sensors. If the surface of the optical fiber is modified, the refractive index varies; for example, if on the surface is fixed a certain receptor able to absorb the evanescent wave, when it comes into contact with the analyte, the refractive index will be different from the previous one (see Figure 2). The presence of a modified surface brings a variation of the conditions for which the evanescent wave is absorbed. When the new conditions are fixed and a decrease in the output intensity is noticed, the analyte has contacted the receptor fixed on the surface [47].

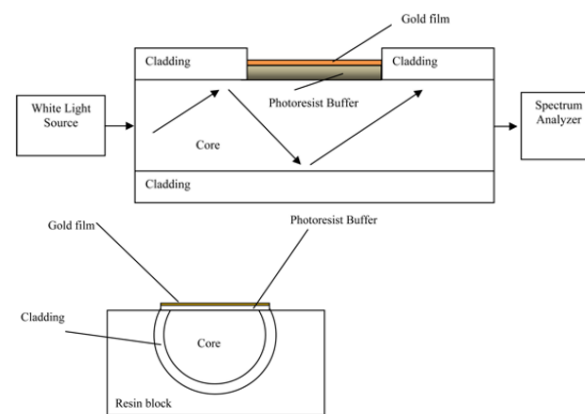


Figure 2. SPR sensor scheme. Reprinted with permission from [48] under an Open Access Creative Commons CC, license 4.0, to MDPI.

If the light hits a thin portion of metal under certain conditions, the generated phenomenon is called surface plasmon resonance (SPR). In this case, the evanescent wave excites the surface plasmons of the metal. The resonance conditions are [48]:

$$K_0 n_c \sin \theta = K_0 \left(\frac{\epsilon_{mr} n_s^2}{\epsilon_{mr} + n_s^2} \right)^{1/2}$$

$$K_0 = \frac{2\pi}{\lambda}$$

Dwivedi et al. [49] described these formulas in a very clear way: “The term on the left-hand side is the propagation constant (K_{inc}) of the evanescent wave generated as a result of attenuated total reflection (ATR), the light incident at an angle θ through a light coupling device (such as a prism or optical fiber) of refractive index n_c . The right-hand term is the surface plasmon wave (SPW) propagation constant (K_{sp}), with ϵ_{mr} as the real part of the metal-dielectric constant (ϵ_m) and n_s as the refractive index of the sensing (dielectric) layer”. The conditions are very sensitive to any small change of the ambient; for this reason, it is challenging to find the right balance among all the parameters. The angle of incidence and wavelength are those variable parameters that we may change to find the right resonance conditions.

In the case of nanoparticles, the effect will be called localized surface plasmon resonance (LSPR). Noble metal nanoparticles are sensitive to electromagnetic waves in the visible light range; the radiation induces a surface polarization of the nanoparticle. If the particle size is similar to the dimension of the penetration layer of the evanescent wave, electrons begin to oscillate in resonance [50]. This effect leads to an intense absorption at that wavelength. The obtained spectrum is strongly influenced by the size and shape of the nanoparticles; for example, particles smaller than the incident wavelength will lead to narrower peaks, while larger particles will lead to wider peaks because the electrons during resonance can go out of phase [50]. Ideally, there is only one LSPR resonance peak in a spherical nanoparticle because the charges within a nanoparticle have only one way to separate. In contrast, if the objects are anisotropic, the charges can separate longitudinally and transversely in-plane and out of plane; this phenomenon leads to the generation of different peaks or shoulders in the spectrum [51].

The LSPR effect of nanoparticles is often exploited due to the presence of very intense and well recognizable signals at certain wavelengths; furthermore, these signals also carry information regarding the shape and size of the nanoparticles (see Figure 3) [52].

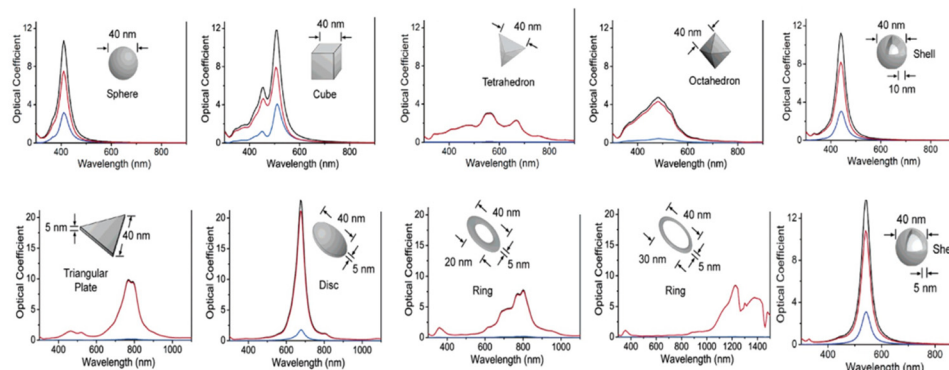


Figure 3. Effects of nanoparticles shape on the absorbance spectrum. Reprinted with permission from [52], copyright 2006, American Chemical Society.

Morphological properties of nanoparticles and the physico-chemical environment surrounding them influence their LSPR and the corresponding spectra. The Mie model can successfully calculate the plasmon resonance spectra of spherical nanoparticles. It is based on the solution of the Maxwell equations in spherical coordinates using the multipoles expansion of the magnetic and electric fields and taking into account the discontinuity of the dielectric constant between the nanosphere and the surrounding medium. Since aggregation can also implicate two or more nanoparticles with non-spherical shapes (mainly spheroids), the overall spectra can be calculated by the Gans model, i.e., the extension of the Mie theory for spheroidal shape nanoparticles [53]. Analytical methods such as the previously summarized Mie and Gans theory are useful to describe only highly symmetric nanoparticle shapes. However, grid-based approaches like discrete dipole approximation (DDA), finite difference time domain (FDTD), and finite element method (FEM) can simulate the plasmonic spectrum of any nanoparticle shape [54].

An attractive property of the surface plasmon wave is that its resonance frequency depends on the dielectric constant (refractive index, RI) of the medium surrounding the nanoparticles. In particular, an increase of the medium RI corresponds to an LSPR redshift. These changes can be useful as optical sensing tools. For example, the binding of the analyte to the recognition site on the nanoparticles, causing the SPR shift due to the local RI change, can be useful for sensing the target analyte. The SPR band shift is desired to be as high as possible in response to small RI changes to get good sensitivity [55].

In conclusion, nanoparticles are widely used in sensor technology thanks to their self-indicating properties such as fluorescence and LSPR effect. Moreover, they can be of interest in other fields; for example, AgNPs have been applied in medicine thanks to their antimicrobial properties; AuNPs are used as indicators for antibodies in some specific analyses [56].

Unfortunately, nanoparticles have shortcomings as well; for example, they can easily enter the environment through water, air or soil and may be dangerous if accumulated in organs or tissues [23]. The following Sections 2.1 and 2.2 summarize the principal synthetic strategies for the preparation of Ag and Au nanoparticles, respectively.

2.1. AgNPs Synthesis

This section presents an overview of AgNP preparation methods by physical, chemical, and biological approaches.

2.1.1. Physical Methods

The physical methods for AgNPs synthesis include the evaporation–condensation and the laser ablation techniques. By both methods, large quantities of AgNPs of high purity can be prepared without using toxic reagents, although agglomeration remains a problem since these methods avoid the employment of capping agents. Moreover, both

strategies are expensive because they require high energy consumption, long procedures and complex equipment.

A gas-phase path is generally used for the evaporation- condensation method, and a tube furnace is applied to synthesize NPs at atmospheric pressure. In particular, a vessel containing the metal source is put in the center of the tube furnace. The metal is let to evaporate into the carrier gas, so obtaining the NPs. The shape, size, and yield of the NPs production can be tuned by changing the reactor's design. However, the AgNPs synthesis by this method shows several drawbacks. The tube furnace occupies a large room of the instrument; the method consumes high energy and requires a long time to maintain a constant temperature. For overcoming these problems, it was demonstrated that a ceramic heater could be efficiently employed.

The other physical method is laser ablation. In this case, a bulk of metal source is placed in a liquid phase. After irradiation with a pulsed laser, the NPs formation takes place. The characteristics of the NPs synthesized by this method depend on different experimental conditions, such as the property of the liquid media, laser power, duration of irradiation, and type of the metal. Unlike chemical methods, the laser ablation synthesis of NPs is not subject to contamination [57].

2.1.2. Chemical Methods

Chemical methods are the most common among the different strategies since they are convenient, efficient, and simple. These methods are generally based on a chemical reduction of aqueous or organic solutions of silver ion salts. Usually, a one-pot synthesis is applied using various reducing agents such as sodium borohydride, sodium citrate, ascorbate, hydrazine, and ammonium formate. The control of the growth of AgNPs is essential for obtaining smaller size nanoparticles with a spherical shape; this can be possible by adding capping agents. These substances are also used to stabilize and avoid agglomeration and oxidation of NPs. Most frequently, capping agents are cellulose chitosan, gluconic acid, or polymers such as polyethylene glycol (PEG), poly N-vinyl-2-pyrrolidone (PVP), polymethacrylic acid (PMAA) or polymethylmethacrylate (PMMA) [58,59].

2.1.3. Green Methods

At present, there is a growing interest in developing environmentally friendly NP synthesis methods. The traditional physical and chemical methods are quite expensive and use hazardous reagents even if they allow the production of NPs with well-defined shapes and pure. Green syntheses that use biomass resources such as plant or plant extracts and biological microorganisms could be an alternative towards eco-sustainability [58].

Several works have recently proposed AgNP syntheses by green approaches using various plant and plant extracts since these biomasses are cheap, available in large quantities, and possess numerous metabolites able to reduce silver(I) salts.

The first method was proposed in 2003 by Gardea-Torresdey et al. using alfalfa sprouts; the roots of this plant can absorb silver ions from an agar medium, then reduce and transfer them into shoots where the Ag atoms are converted in AgNPs [60].

Later, several other plants were reported to promote AgNP syntheses. The synthetic approach involved collecting the plant part of the interest; then, it must be washed thoroughly to remove necrotic plant, epiphytes, and, eventually, debris. The clean material is dried for a couple of weeks and then powered by using a simple household blender. A portion of about 10 g of the powder was boiled with 0.1 L of distilled water, in general, using a hot percolation method. Then, the infusion must be filtered to obtain a clear extract solution. A few mL of this plant extract, a solution of AgNO₃ 1 mM was added, and the conversion Ag(I) → Ag(0)-NPs can be monitored by UV-vis spectrophotometric analysis [61].

According to several reviews, in the AgNPs synthesis mediated by plant and plant extract, alcohols, aldehydes, phenols and flavonoids act as reductants and capping agents.

In the most recent studies, AgNPs were synthesized, for example, from extracts of *Bunium persicum* seeds, *Hamamelis virginiana*, *Rubus ellipticus* and *Psychotria nilgiriensis* leaves, or tamarind fruit [58].

As well known, microorganisms such as fungi and bacteria, are very helpful in the environmental remediation of inorganic contaminants, being able to reduce metal ions. Several bacteria can synthesize AgNPs intracellularly since their intracellular components act as reducing and/or stabilizing agents [57].

For these syntheses, fungi are most interesting than bacteria since they secrete higher amounts of protein that can amplify the production of NPs, making the scale-up and downstream process very simple and cheap [58].

One of the first examples of fungi-mediated NPs synthesis is that reported by Mukherjee et al. [62]. They proposed the synthesis of AgNPs using the fungus *Verticillium*. Contacting the fungal biomass with an aqueous solution of silver(I) ions results in an intracellular reduction of Ag^+ with the formation of AgNPs of about 25 nm. Electron microscopy analyses of a thin section of the fungal cells showed that nanoparticles were formed under the surface of the cell wall, probably because of the reduction of Ag^+ by enzymes in the cellular membrane [63].

Unfortunately, several filamentous fungi that have been reported for extracellular biomass-free syntheses of silver nanoparticles are pathogenic to humans and/or plants, so this makes tricky manipulation and disposal of the biomass, limiting the commercialization of the synthesis method. In this regard, recently, green approaches using nonpathogenic fungi are being developed [63].

2.2. AuNPs Synthesis

Several methods for synthesizing AuNPs, based on top-down and bottom-up procedures, have been proposed so far. This section summarizes the AuNP synthetic methods based on physical, chemical, and green approaches.

2.2.1. Physical Methods

The physical approaches comprise sonochemical, γ -irradiation, microwave irradiation and UV radiation methods, laser ablation techniques and thermolytic and photochemical processes.

With the synthesis based on γ -irradiation high purity AuNPs of controllable size ranging from 5 to 40 nm can be achieved. The sonochemical procedure permits the synthesis of bimetallic Au-Pd nanoparticles and the inclusion of AuNPs in the pores of silica-based materials. In thermolytic and UV processes, high temperature and ultraviolet radiations act as reducing agents in AuNPs production, and by optimization of these processes, the control of the NPs dimensions was obtained. The synthesis by laser ablation was generally performed by reduction of HAuCl_4 photo-induced by a laser beam at 532 nm and permitted the preparation of AuNPs with tunable characteristics [64].

2.2.2. Chemical Methods

Chemical methods of AuNPs are the most frequent. They require mild or strong reducing agents, such as citrate, sodium borohydride or hydrazine, for starting the process and promoting the nucleation of nanoparticles.

Among the syntheses of AuNPs, the Turkevich method [34] is one of the most used thanks to its simplicity and capability in synthesizing very stable nanoparticles of defined shape and size. The synthesis consisted of the chemical reduction of HAuCl_4 by citrate solution. The description of this procedure is reported above.

Although hydrazine and NaBH_4 are very effective reducing agents and have been frequently applied, they are environmentally and biologically toxic, so green approaches are becoming the most developed for nanoparticles synthesis [65].

2.2.3. Green Methods

The green approach is becoming an interesting direction for NPs syntheses to overcome the environmental and toxicity problems caused by chemical and physical methods. In Nature several biological sources that can be successfully revalued during the synthesis of AuNPs, such as plants, algae, bacteria and fungi are available [66,67].

For example, polyphenolic compounds in tea leaves, i.e., flavins and catechins, were proposed as reducing and capping agents in AuNPs synthesis. These compounds demonstrated outstanding properties as initiators and stabilizers, permitting the preparation of 15–40 nm AuNPs [68]. Phytochemical constituents of cumins, such as alcohols, aldehydes, and fats, containing hydroxyl, carboxyl, thiol and amine functional groups, were used as reducing agents in AuNPs preparation. Here, arabic gum is added as a stabilizer [69].

AuNPs can also be green synthesized by using bacteria and fungi. An interesting study proposed a method for producing stable and monodisperse AuNPs of dimension about 10 nm by adding HAuCl₄ solution to whole cells of the marine bacterium *Marinobacter Pelagius* [70].

Another green approach to AuNPs synthesis was proposed by Mukherjee et al., using the fungus *Fusarium oxysporum*. When added to an aqueous solution of HAuCl₄ ions, the reductase enzymes released by the fungi reduced the metal ion, leading to an extracellular formation of AuNPs. The author demonstrated that the prepared nanoparticles were smaller and more monodisperse than those synthesized intracellularly with bacteria [71].

3. Ag Nanoparticles-Based Colorimetric Sensors

Au and Ag nanoparticles have been widely applied in colorimetric detection thanks to their enhanced LSPR optical property. Although AgNPs have been less used than AuNPs in colorimetric assays, very interesting works have been published regarding sensors based on aggregation, etching and growth of AgNPs. In this section, some examples of colorimetric sensors will be described [72].

3.1. Colorimetric Sensors Based on AgNP Aggregation

3.1.1. Metal Ions Detection

An application of AgNPs for sensing Pb(II) ions after its complexation with dithizone was recently reported. Dithizone is a selective dye that forms stable complexes with lead and other divalent cations at pH around 6; it also has a sulfide group able to covalently bond metallic AgNPs. In this study, the Ag nanoparticles were added to a solution containing Pb(II)-dithizone complex. AgNPs aggregate after contact with Pb(II)-dithizone complex; consequently, their LSPR absorbance at 421 nm decreases; this variation is applied to detect lead(II) indirectly. The perspective of the method is its application to environmental and biological samples for a selective, sensitive, and rapid sensing of Pb²⁺ [73].

Again for lead(II), Khan et al. proposed a low-cost and simple colorimetric sensor based on AgNPs obtained from the leaf extract of *Aconitum violaceum*, a perennial plant species present in the Himalayan region of Pakistan, India, and Nepal. AgNPs have been proficiently synthesized thanks to the presence of a significant quantity of polyphenols in the extract. The so prepared AgNPs were used as a colorimetric sensor for Pb²⁺. In fact, in the presence of lead(II), the nanoparticles evidenced a color change from yellow to red; this variation was monitored by UV-vis spectroscopy. Furthermore, the sensor showed good linearity being a concentration range of 0.5–25 µM and a detection limit of about 0.1 µM [74].

Recently another low-cost and selective sensor for determining lead(II) in waters and wastewater samples was presented. In particular, a plasmonic colorimetric sensing strategy was applied using AgNPs modified with polyvinyl alcohol (PVA) and paper-based analytical devices (PADs). The procedure consisted of measuring by a UV-vis spectrophotometer the redshift of the LSPR absorption band of AgNPs/PVA in the visible region after adding Pb(II); moreover, the color intensity of PADs was recorded with a smartphone and processing the data by ImageJ software. The mechanism of color change

due to the red shift from 410 nm to 550 nm resulted from the strong ion-dipole interaction of Pb(II) with AgNPs/PVA that perturb the stability of the nanoparticles, causing their aggregation. The calibration curve showed pretty good linearity from 20 to 1000 μgL^{-1} and a limit of detection of 8 μgL^{-1} by UV-vis spectrophotometric measurements; while a linear range from 50 to 1000 μgL^{-1} and a LOD value of 20 μgL^{-1} were obtained by PADs [75].

An attractive work reported a selective and low-cost colorimetric sensor for detecting Pb²⁺ and Hg²⁺ using AgNPs obtained by a green synthesis mediated by a roots extract of *Bistorta amplexicaulis*. The color change of AgNPs from dark-brown to light yellow for Hg²⁺ and to light brown for Pb²⁺ is due to the complexation and aggregation of AgNPs in solution. Thus, this colorimetric sensor offers qualitative and quantitative information simply by naked-eye detection, without using expensive instruments; moreover, it is very sensitive for Pb²⁺ and Hg²⁺, presenting a detection limit of 0.2 μM and 0.8 μM for Pb²⁺ and Hg²⁺, respectively [76].

Kumar et al. developed a photoinduced synthesis of very stable AgNPs using, as a reducing and stabilizing agent, an aqueous extract of *Murraya koenigii*. The so synthesized nanoparticles were applied for the colorimetric detection of Hg²⁺; a linear correlation between surface plasmon resonance (SPR) band intensity and increasing concentrations of Hg²⁺ was observed (with a linear range from 50 nM to 500 μM). This behavior was explained considering an oxidation-reduction mechanism: by adding Hg²⁺ into the AgNPs solution, the AgNPs are oxidized to Ag⁺ and, accordingly, Hg²⁺ ions are reduced to Hg⁰. In fact, after the addition of Hg²⁺, the dark brown color of the AgNPs solution disappeared and the SPR band intensity diminished with minor shifting towards the blue region [77].

Dong et al. proposed a very sensitive and selective colorimetric method for determining Cd(II) by applying AgNPs capped with chalcone carboxylic acid. In the presence of Cd(II), the formation of a complex with CAA occurs, followed by particles aggregation and color variation from yellow to orange (i.e., the sorption peak shifts from 396 to 522 nm). The selective determination of Cd(II) was obtained since other cations such as Al(III), Fe(III), Cr(III), Co(II), Ca(II), Mg(II), Cu(II), Mn(II), Ni(II), Pb(II), Hg(II), and Zn(II), do not interfere significantly. The limit of detection is about 0.1 μM . This method was applied to determine Cd(II) in natural waters, and the results obtained agreed with those achieved by ICP-OES analysis [78].

A simple colorimetric method using citrate-stabilized AgNPs for Ni(II) determination in waters was recently proposed. Sodium borohydride was used as a reducing agent and trisodium citrate as a stabilizer for the nanoparticle synthesis. Citrate-capped silver nanoparticles show a yellow color in solution provoked by the excitation of the local surface plasmon resonance band around 400 nm. Upon addition of Ni(II), almost immediately, a color change of the citrate-stabilized AgNPs from yellow to deep orange was observed; this variation was explained considering the particles aggregations due to the interaction between the Ni(II) ions with the carboxylic group present on the surface of the nanoparticles (see Figure 4). A calibration curve linear from 0.7 to 1.6 mM Ni(II) concentration was obtained; the LOD and LOQ were 0.75 and 1.52 mM, respectively. Before the application of the method to real samples, interference studies were performed testing some representative cations such as Ag(I), Li(I), Ca(II), and Mg(II); the method showed excellent selectivity for Ni(II) compared to the other metal ions. Lastly, the method was applied for determining Ni(II) in synthetic solutions and tap waters, giving pretty good results [79].

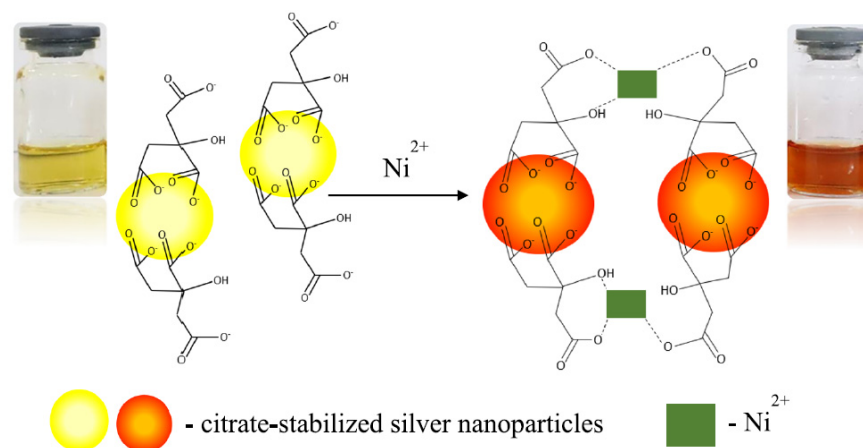


Figure 4. Colour change of the citrated capped AgNPs due to the particles aggregations caused by the interaction between the Ni(II) ions with the carboxylic group present on the surface of the nanoparticles. Reprinted with permission from [79], under an Open Access Creative Common CC to Springer Nature.

An economical and eco-friendly method based on AgNPs for sensing Al(III) was presented. In particular, organic functional groups present in *Mentha arvensis* plant extract are used as reductants and stabilizers in the synthesis of AgNPs, and also they provide a suitable active site for selective and sensitive Al(III) sensing. The presence of Al(III) in solution induced nanoparticles aggregation followed by a color change from yellow to reddish-brown. The modified AgNPs show high Al(III) sensitivity, and the calibration curve is linear from 200 to 1 nM metal ion concentration. This method was successfully applied for Al(III) detection in water samples where the cation was present at the nanomolar concentrations [80].

Green synthesized AgNPs from *Moringa oleifera* bark extract were prepared as sensitive Cu(II) sensors. The *Moringa oleifera* plant contains amino acids, fatty acids, vitamins, and phenolics compounds; of these substances, glucosinolates are the most crucial functional groups thanks to their complexation properties towards metal cations. The change of the nanoparticles' surface plasmon resonance (SPR) spectrum was studied by varying Cu(II) quantities, and a color change from brown to gray was verified. This variation is due to Cu(II) complexation by the benzyl glucosinolate present in *Moringa oleifera*. A linear relationship absorbance vs. Cu(II) concentration in the range 10–90 μM was observed. The sensor's selectivity towards Cu(II) was also verified since only small changes of the SPR band were registered in the presence of other different cations (i.e., chromium, mercury, zinc, and nickel) [81].

3.1.2. Pharmaceuticals, Biomolecules, and Environmental Contaminants Detection

A dual fluorescence-colorimetric assay for determining the antipsychotic drug olanzapine using Rhodamine B modified AgNPs was developed. The natural fluorescence of Rhodamine B was quenched upon reaction with AgNPs capped with citrate. Adding olanzapine to Rhodamine B-AgNPs, the analyte replaced the surface-bound Rhodamine B molecules, the aggregation of the nanoparticles occurred, corresponding fluorescence reappeared, and a colorimetric variation was observed. By fluorescence measurements, a linear concentration range of olanzapine from 0.05 to 10 μM was obtained; on the other hand, the colorimetric response is linear from 5.0 to 50 μM olanzapine concentration. The LOD values obtained by fluorescence and colorimetric measures were 0.013 μM and 1.25 μM , respectively. The good selectivity for olanzapine in the presence of other antipsychotic drugs, sugars, amino acids and cations, was demonstrated. Moreover, the assay was applied to determine olanzapine in pharmaceutical formulations and in a pharmacokinetic study of the drug in rats [82].

2-Mercaptoethylamine, or simply cysteamine, is an aminothiols drug used in different clinical treatments, such as for cystinosis, Parkinson's and Huntington's neurodegenerative diseases and also applied as a neuroprotective agent. A recent work presents a colorimetric method for determining cysteamine based on the application of polyvinylpyrrolidone-capped AgNPs. Poly(vinylpyrrolidone) is a polymer widely employed in NP synthesis since it acts as a protective agent preventing nanoparticle aggregation. The sensing properties of PVP-AgNPs toward cysteamine were evaluated in aqueous solutions. In the absence of cysteamine, the suspension of the nanoparticle remained pale yellow colored with the characteristic SPR band at 395 nm. Increasing the cysteamine concentration from 0.2 to 2.0 μM , the peak intensity at 395 nm decreased, and a significant bathochromic shift from 395 to 436 nm was observed with the appearance of a new peak at around 560 nm. Simultaneously, a color change from pale yellow to purple appeared due to the nanoparticles' aggregation upon the addition of cysteamine. The good selectivity of the sensor was tested considering several interfering compounds. Thanks to the promising results, the method was successfully applied to detect cysteamine in serum samples, suggesting its potential for biomedical analysis [83].

In human physiology, urinary creatinine concentration is crucial since it is used to evaluate the renal function and diagnose possible diseases. In an interesting study, citrate-capped AgNPs were used as sensors for the colorimetric determination of creatinine in human urine. The detection mechanism bases on the creatinine-mediated aggregation of the citrate-capped silver nanoparticles at pH 12, which produces a detectable color change. This sensor showed a linear response from 0 to 4.2 μM creatinine concentration with a LOD of 53.4 nM. This method does not require further surface functionalization of the silver nanoparticles or sample pretreatment, so the advantages of simplicity, coupled with good sensitivity and selectivity, highlight its utility as a promising tool for creatinine monitoring in low-resource, point-of-care settings [84].

The determination of arginine is very important since, in the human body, it leads to different effects such as modulation of immune function, insulin sensitivity, vascular tone, hormone secretion, and endothelial function. Arginine is also applied to detoxify the blood ammonia, and it is also involved in many pathways. A recent study reported a method for the quantification of arginine by using Ag NPs. In particular, Ag NPs conjugated with arginine reacting with an excess of Pb^{2+} ions forming a complex; this reaction leads to color variation of the nanoparticles from brownish yellow to black. A linear relationship absorbance vs. concentration was observed from 1 nM to 1 mM arginine concentration; the LOD value is around 0.1 nM [85].

A recent work presents an optical sensor for adenosine analysis in human urine. The sensor consists of AgNPs functionalized with an anti-adenosine aptamer as a sensing probe. The sensor response depended on the different stability of anti-adenosine aptamer-AgNPs in the presence of adenosine; in particular, the nanoparticles' aggregation was gradually reduced by the increase of adenosine concentration. The method permitted the adenosine determination in a concentration range from 60 to 280 nM with a LOD of 21 nM. The reliability of the assay was established by detecting adenosine in urine samples of two lung cancer patients; the percentage of recoveries ranged from 98 to 107% [86].

An interesting H_2S sensor based on gellan gum-stabilized AgNPs was developed for a real-time monitor of meat spoilage for intelligent packaging. The employment of AgNPs as the hydrogen sulfide sensor was due to the high reactivity of Ag with H_2S to form the salt Ag_2S , which caused notable LSPR changes of AgNPs. Moreover, the AgNPs were obtained using the linear exopolysaccharide gellan gum as a stabilizer and reducing agent for obtaining good nanoparticles' stability during storage. Gellan gum is edible and has received U.S. FDA and EU (E418) approval for its use as gelling, suspending and stabilizing agent in various foods. The so prepared sensor can monitor meat spoilage in situ and in real-time since it can be part of an intelligent packaging system. In particular, a gellan gum-AgNPs hydrogel instead of the usual nanoparticle solution was used in meat packages. The hydrogel was prepared by adding agar into the nanoparticle solution. H_2S

can permeate into the hydrogel, and its concentration increases with the exposure time until saturation. The sensor was applied to monitor chicken breast and silver carp spoilage with excellent results. Therefore, it can be used as a portable and low-cost H₂S sensor for accessible and instrument-free monitoring of meat spoilage in intelligent packaging [87].

As well known, pesticides are substances employed to repel, kill, or control some forms of plant or animal life that are considered to be pests. Pesticides can cause short-term adverse health effects and chronic effects that can arise months or years after exposure. Some examples of chronic diseases are immunotoxicity, endocrine system disruption, cancers, congenital disabilities, and neurological pathologies. Therefore, new methods or tools are necessary to forecast the potential dangers of pesticides and thus reduce the adverse effects on the environment and human health [88].

In this regard, a colorimetric method for sensitive and selective determination of the fungicide tricyclazole based on fluorescein-functionalized AgNPs was presented. The addition of tricyclazole to the functionalized nanoparticles induced the absorbance at 394 nm decrease and the evident color change from yellow to gray due to the aggregation of the nanoparticles. The selectivity of the assay was tested by analyzing the UV-vis spectrum of the functionalized nanoparticles in the presence of other pesticides (acetamiprid, bifenthrin, carbaryl, carbofuran, chlorpyrifos, clothianidin, 2,4-D, dichlorvos, dicofol, fenvalerate, glyphosate, glufosinateammonium, kresoxim-methyl, imidacloprid, methomyl, pencycuron, profenofos, propanil, thiodicarb, trichlorfon). The test results showed that the interferences did not cause the nanoparticles' aggregation, and the only tricyclazole induced the color change and thus the variation of the UV-vis spectrum of the nanoparticles. The recoveries of the tricyclazole in spiked rice samples were from 94.6% to 103.0%, and a LOD of about 0.051 mg/L [89].

Phoxim (O,O diethyl-O- α -oximinophenyl cyanophosphorothioate) is an effective broad spectrum insecticide. An interesting study proposed a green synthesis of carbon dots-modified silver nanoparticles (CDs-modified AgNPs); NaBH₄ was used as a reducing agent and carbon dots as stabilizing agents. In solution at pH 6, the presence of phoxim induced the aggregation of the dispersed CDs-modified AgNPs and the consequent color change from yellow to red (see Figure 5) due to the redshift of the SPR peak from 400 to 525 nm. The developed assay was applied to the phoxim detection in river waters, tap waters and apples with good recovery in the range of 87–110.0%. The LOD of the method is about 0.04 μ M. Thanks to the sensitivity and selectivity performances, the sensor can be successfully applied to analyze environmental and food samples [90].

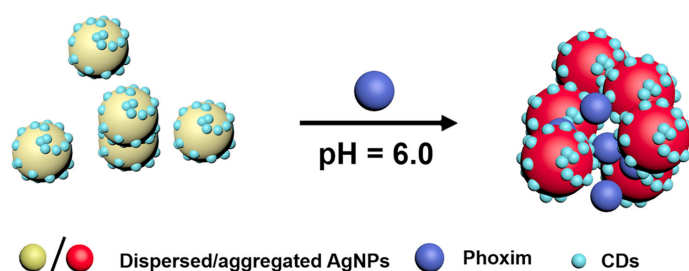


Figure 5. Scheme of the detection mechanism of Phoxim by CDs-modified AgNPs. Reprinted with permission from [90], copyright 2018 Elsevier B.V.

A one-pot microwave production of AgNPs from mature stem extract of the plant *Coscinium fenestratum* and AgNO₃ was studied to develop a spectrophotometric sensor for the dithiocarbamate fungicide thiram. The stem plant extract also acted as a stabilizing agent of the nanoparticles. Thiram is a non-systemic fungicide commonly used in agriculture in the cultivation of fruit plants. The addition of thiram to a solution of the produced nanoparticles induced a change in the SPR peak at 423 nm. A decrease of the peak was observed in a thiram concentration range from 10 to 90 μ M. This behavior was explained considering the intermolecular H-bonding interactions between thiram and the

functional groups present in the capping agent. The sensor's selectivity was evaluated considering as potential interferents the macro constituents of water samples; since the only few changes observed, the selectivity of the nanoparticles toward thiram was proved. A limit of detection of about 0.18 mg/L, lower than the limit value of 7 mg/L proposed by US-EPA, was obtained; so that this method can be promising to detect thiram in natural water and environmental samples [91].

3.2. Colorimetric Sensors Based on AgNPs Anti-Aggregation

Although most colorimetric sensors are based on AgNPs aggregation, this approach faces some difficulties, such as the lack of stability and selectivity since many external factors can induce AgNPs aggregation. On the contrary, the anti-aggregation-based devices strategy could improve selectivity lowering the possibility of false-positive responses [92].

Recently, a fluoride sensor based on the anti-aggregation of modified silver nanoparticles was developed. In particular, aggregated AgNPs were prepared using sulphanyl acid and catechol as stabilizing-reducing agents (SA-CAT-AgNPs). The presence of fluoride induced a color change of the aggregated nanoparticles solution from red to yellow, proportional to the fluoride concentration in the range from 1 to 40 μM with a LOD of 0.2 μM . The color variation was ascribed to the anti-aggregation of SA-CAT-AgNPs due to the adsorption of fluoride ions on the AgNPs surface and the simultaneous release of the SA-CAT capping agent. The sensor was applied for fluoride detection in Iranian spring waters. The results were not significantly different from those achieved by the standard potentiometric method with the ion-selective electrode, suggesting that the method can be promising for fluoride detection in natural waters [92].

Chavada et al. proposed a colorimetric method for determining the concentration of deferiprone, an iron-chelating drug, based on AgNPs functionalized with pyrophosphate groups. The so obtained nanoparticles aggregated in the presence of iron(III) ions inducing the solution color change from yellow to red. After adding increasing quantities of deferiprone, the color of the nanoparticle solution turned yellow due to the anti-aggregation process, and the intensity of this variation was proportional to the deferiprone concentration. The method gave a linear response from 6.0–100 μM deferiprone concentration and a LOD of 0.28 μM . The selectivity was verified since no responses were obtained in the presence of many amino acids, saccharides, and inorganic ions. The method was applied for determining deferiprone in commercial drugs and a spiked human plasma demonstrating good accuracy, so this innovative and cheap assay can be promising for deferiprone dosage in biological fluids and pharmaceuticals [93].

Cheap and rapid assays for detecting bacteria are of huge importance. An interesting work proposed a colorimetric method for determining gram-negative bacteria (here, *E. coli* was used as a model). It is based on the anti-aggregation of 4-mercaptophenylboronic acid-functionalized silver nanoparticles (MPBA-AgNPs). MPBA is one of the boronic acid derivatives; it could interact with *cis*-diol groups present in the saccharide part of bacteria cells; so that it can be efficiently used as the recognition system in sensors devoted to bacterial detection. In the proposed method, the MPBA-AgNPs' aggregation was inhibited by bacterial cells, and a consequent color change, from yellow to brown, was revealed. The dynamic range was between 5×10^4 cfu/mL and 10^7 cfu/mL *E. coli* and the LOD of 9×10^3 cfu/mL was achieved. The sensor response is fast, requiring about 20 min. The feasibility of the assay in real samples analyses was verified by detecting *E. coli* in tap water spiked with different concentrations of bacteria (0.5×10^6 , 10^6 , 5×10^6 cfu/mL), obtaining pretty good recovering (from 93 to 107%) and standard errors below the 4% [94].

3.3. Colorimetric Sensors Based on AgNPs Etching

The study of several metal nanoparticle sizes, shapes, and clusters highlighted the importance of these parameters to customize the plasmonic characteristics of the nanomaterials. The development of chemical methods able to simultaneously control particle shape, size, and composition at the nanoscale level is fundamental. For example, a simple

chemical etchant can be used to produce complex nanoparticles architectures. Figure 6 shows the change of UV-vis-NIR spectra caused by the etching of octahedra AgNPs during the reaction upon adding particles to the etching solution. The color changed from tan to yellow, orange, purple and finally reddish-pink [95].

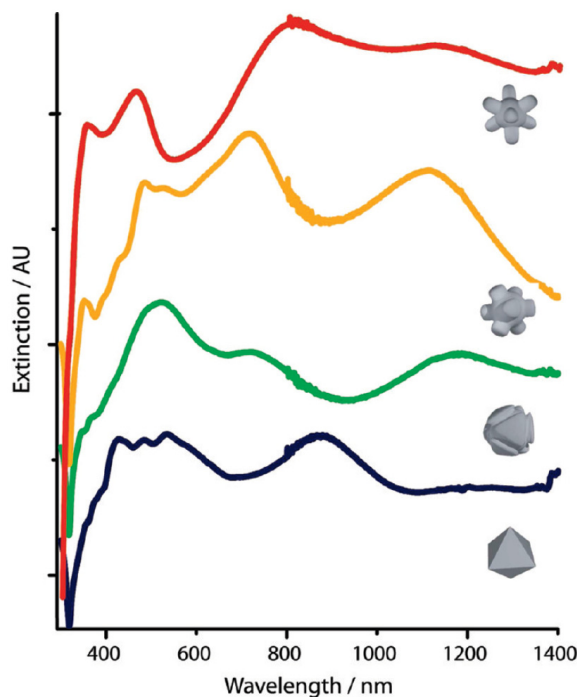


Figure 6. UV-vis-NIR spectra of AgNPs during an etching process starting from octahedral-shaped particles. Etchant solution: $\text{H}_2\text{O}_2/\text{NH}_4\text{OH}/\text{CrO}_3$ in a 1:5:0.08 ratio. Reprinted with permission from [95], copyright 2010, American Chemical Society.

The color change induced by the etching of AgNPs is one of the strategies adopted in developing colorimetric sensors. An interesting study presented a colorimetric assay for the detection of uric acid based on the suppression of oxidative etching of AgNPs by chloroauric acid [96]. The etching occurs thanks to the oxidation of the Ag(0) to Ag(I) by HAuCl_4 ; consequently, Au(III) is reduced to Au(0) and deposits onto the silver surface, so forming Au-AgNPs with honeycomb shape evident for the color change from yellow to brown. In the presence of uric acid, the oxidization etching of AgNPs is inhibited; accordingly, the brown color disappears, and the absorbance peak is blue-shifted from 477 to 428 nm. This process has been exploited to develop the colorimetric sensor. A LOD of the method of about 30 pM, and a linear response range from 0.1 nM to 0.1 mM uric acid concentration, were reported. The trustworthiness of the method was successfully demonstrated by analyzing spiked serum samples since the results obtained were non significantly different from those achieved by a routine clinical method. Thanks to the excellent results, the sensors could be employed for medical diagnosis.

A similar approach was applied to develop a colorimetric sensor for captopril, an angiotensin-converting enzyme (ACE) inhibitor prescribed for the clinical treatment of hypertension, heart failure and for preventing kidney failure due to high blood pressure and diabetes [97]. The sensing is based on tuning the localized surface plasmon resonance (LSPR) of triangular Ag nanoprisms by oxidative etching induced by Cl^- ions. In particular, a gradually blue shift from 660 to 420 nm occurred by increasing the chloride concentration, and consequently, a color change from blue to yellow arose; this is due to the transformation of the triangular-shaped nanoprisms in the smaller disc-shaped Ag nanoparticles. When captopril was added, it was bound on the Ag nanoprisms surface through an Ag-S bond involving the thiol group of the drug. Thereby captopril prevented the nanoprisms etching. Based on this process, a colorimetric assay was proposed for the quantitative detection of

captopril, with a linear response range from 10 to 600 nM. A drawback is that biothiols can respond to the sensor and generate interference so that the method could be applied for quality control of captopril in pharmaceutical products, but it is not suitable for biological fluids analysis where interfering thiols may exist.

A plasmonic ELISA method based on the oxidative etching of Ag nanoprisms for the detection of danofloxacin, a fluoroquinolone antibiotic, was recently proposed [98]. The method combines localized surface plasmon resonance (LSPR) of nanoparticles with the classical ELISA technique. It is based on glucose oxidase-catalyzed glucose degradation to etch the Ag nanoprisms, using an indirect competitive procedure. In Figure 7, a scheme of the method is shown. In the absence of danofloxacin (DAN) molecules in the sample, the DAN monoclonal antibody linked to the biotin (biotin-mAb) can interact directly with the conjugate DAN/bovine serum albumin (DAN-BSA) coating the microplates. Then, the biotinylated GOx (biotin-GOx) was captured by biotin-mAb through the mediator streptavidin (SA). Successively, glucose was added, and reacting with biotin-Gox, produced H_2O_2 , which caused the nanoprisms etching. The etching converted the nanoprisms to nanodisks with a corresponding solution color change from dark blue to colorless. On the contrary, in the presence of DAN, the fluoroquinolone molecules were competitively bound to biotin-mAb and inhibited its binding to the DAN-BSA coating. In this case, no H_2O_2 was produced; thus, the solution persisted blue since the nanoprisms retained their morphology. The calibration curve showed a linear range from 0.31 to 10 ng/mL of DAN with a LOD of about 0.2 ng/mL. The proposed method presented good selectivity, accuracy and precision for the danofloxacin determination, so this assay is promising for food safety analysis.

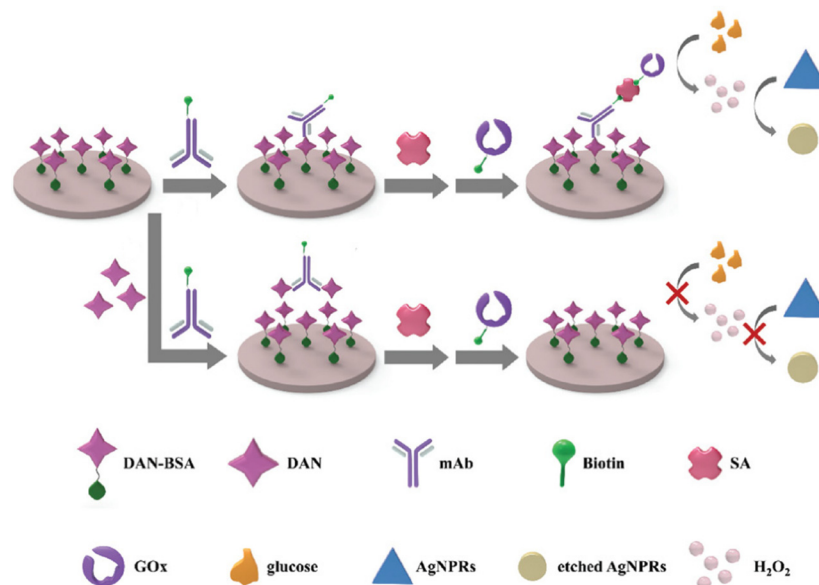


Figure 7. Scheme of the Ag nanoprisms-etching ELISA method for the detection of danofloxacin. Reprinted with permission from [98], copyright 2012, Royal Society of Chemistry.

An interesting study demonstrated that AgNPs solutions could be used as a bifunctional probe, i.e., a colorimetric H_2O_2 chemosensor and a cholesterol biosensor [99]. The sensor's principle is based on the redox reaction between AgNPs and H_2O_2 , which leads to the formation of Ag(0). The nanoparticles' etching and the consequent color change from yellow to pinkish (or colorless depending on the amount of H_2O_2) were observed. A selective and sensitive H_2O_2 detection was obtained with LOD of about 3.5 μ M. Afterward, a colorimetric biosensor was developed for cholesterol determination by combining AgNPs and the cholesterol oxidase enzyme (ChOx). ChOx oxidizes cholesterol into cholest-4-en-3-one and H_2O_2 . Then, the H_2O_2 concentration, detected by the AgNPs etching, reflected the cholesterol level in the sample. This biosensor presented high selectivity and sensitivity for cholesterol detection with a LOD of about 40 μ M; it could be efficiently applied to dose

cholesterol in serum samples, so the bifunctional probe was promising for determining both oxygen peroxide and cholesterol in biological samples, and it is suitable for clinical and medical applications.

3.4. Colorimetric Sensors Based on AgNPs Anti-Etching

Some new recent works have proposed colorimetric assays based on anti-etching of silver nanoobjects. An interesting example is that proposed by Fang et al. The authors described a colorimetric method for determining dopamine in serum, based on the protection of the silver nanoprisms etching induced by Cl^- ions when adding dopamine. Indeed, in the absence of dopamine, chloride ions tend to attach to the edges and angles of the Ag nanoprisms forming Ag-Cl bounds and etching the nanoprisms in nanodisks followed by a color change from blue to yellow. In the presence of dopamine, the catechol group of this molecule was quickly adsorbed onto the silver nanoprisms' surface; so dopamine acted as a protective agent toward the nanoparticles' etching induced by Cl^- . The anti-etching process induced a color variation proportional to the dopamine concentration in the range between 0.5 to 100 nM, The LOD of the method was about 0.16 nM. The applicability of the assay was verified by analyzing human serum samples fortified with dopamine, obtaining good recovery, ranging from 97 to 105%; these results, along with the rapidity, ease of performance and selectivity, make the method promising for biological analyses [100].

Another work, inspired by the previously described one, proposed a colorimetric method for Hg(II) ions detection based on anti-etching of triangular silver nanoplates. In the absence of Hg(II), the triangular nanoplates are etched to nanodisks in the presence of chloride ions, followed by a color change from blue to yellow. In the presence of Hg(II) ions, an amalgam Ag/Hg was formed due to the adsorption and the consequent reduction of mercury ions; an evident color change from yellow to brown, purple, and blue was obtained proportionally to the amount of Hg(II) in solution. The method showed a linear response from 5 nM to 100 nM Hg(II) concentrations with a LOD of about 0.35 nM. The method's validation was achieved by analyzing certified material and river water samples, comparing the obtained results with those achieved by classical chromatography methods [101].

Recently a colorimetric assay for detecting biothiols was presented. It is based on the anti-etching of silver nanoprisms. In particular, a double function of biothiols as anti-etching and aggregating agents for the nanoprisms was observed. At pH higher than 5 and in the absence of biothiols, silver nanoprisms can be etched by chloride ions to give spherical AgNPs and a correspondent color change from purple/blue to yellow. Adding biothiols to the nanoobject solutions, the Ag-S interaction prevents the nanoparticles' etching, and the color returns purple/blue. It was also demonstrated that the individual biothiols homocysteine, cysteine, and glutathione, also exerted an aggregation effect that can be tuned by changing the solution pH. The method was applied to determine the total amount of biothiols in human serum samples; the method's accuracy and rapidity, convenience, and direct determination make the assay promising for biological analysis [102].

3.5. Colorimetric Sensors Based on AgNP Growth

Ag^+ can be used as precursors for AgNPs in growth-based colorimetric sensors; seeds are also sometimes used to grow nanoparticles. For example, a fluorometric method for determining sulfadiazine (a common sulfonamide antibacterial widely used in veterinary medicine to treat infectious diseases) based on the growth of AgNPs on graphene quantum dots was recently proposed [103]. Ag-NPs on graphene quantum dots (AgNPs-GQDs) were synthesized by reduction of silver nitrate with sodium borohydride in the presence of the graphene quantum dots. The quenching of the blue fluorescence of the GQDs (emission maximum peak at 470 nm) was caused by the growth of the nanoparticle on the quantum dots' surface. The addition of sulfadiazine and its interaction with AgNPs restored the fluorescence. The fluorescence increased linearly by sulfadiazine additions in a concentration range from 0.04 to 22.0 μM . LOD and LOQ were found to be 10 and 37 nmol/L sulfadiazine,

respectively. Since the good selectivity, rapidity, and high sensitivity, the method could be promising for determining sulfadiazine in biofluids and complicated matrices.

Another interesting and very recent work presented a colorimetric sensor for *p*-aminophenol based on seed-mediated growth of silver nanoparticles [104]. *p*-Aminophenol is an organic compound classified as nephrotoxic and teratogenic. It is a building block used in several organic and industrial syntheses, and it is the final intermediate in the industrial preparation of paracetamol. *p*-Aminophenol in urine is one of the markers for evaluating the exposure of carcinogenic aniline compounds, and it is also present as the main impurity in paracetamol-based drugs. Thus, accurate methods for quantifying *p*-aminophenol in urine samples and paracetamol-based drugs is of paramount interest. This study proposed a colorimetric sensor based on the capability of *p*-aminophenol to reduce Ag^+ ions, thus enhancing the growth of AgNPs. A solution containing AgNPs as seeds, AgNO_3 and a small amount of NaBH_4 was prepared for obtaining the AgNPs– Ag^+ mixture. After adding *p*-aminophenol to the AgNPs– Ag^+ mixture, further growth of AgNPs was observed by the color change from yellow to orange. The sensor provides good sensitivity and selectivity, with LOD of 15 and 0.32 μM by naked eyes and UV-vis spectrometry, respectively. The good precision and high recovery % were demonstrated by analyzing different human urine samples and the drug Panadol.

4. Au Nanoparticle-Based Colorimetric Sensors

Gold nanoparticles (AuNPs) can be efficiently applied to develop colorimetric sensors since they can be simply functionalized, showing different colors depending on their shape, size, and aggregation state. In the last decade, various sensors were developed, taking advantage of the nanoparticle's color changes in the presence of different analytes.

Recently, novel colorimetric sensors based on the changes of nanoparticles morphology have been developed. In particular, the evolution of AuNPs' shape can be due to etching or growth. So, the changes in the nanoparticles' size, shape and composition, induced by the analytes, are followed by a shift in the SPR band, and a color change appears [105].

In this section, recent applications of AuNPs in colorimetric sensors are discussed.

4.1. Colorimetric Sensors Based on AuNPs Aggregation

Aggregation of AuNPs promoted by analytes is the key point to prepare these sensors. The interaction between analytes and nanoparticles can be obtained by functionalization of the AuNP_s with specific ligands. Typical examples of colorimetric sensors based on AuNP aggregation are those for metal ions; they have been applied in different fields such as environmental, clinical and food analysis. To this end, chelating ligands containing carboxylic, hydroxyl and amino groups are linked to the nanoparticles' surface. The so functionalized AuNPs, in the presence of metal ions, aggregate thanks to the formation of metal ion/ligands complexes, with a resulting color change from red to purple [106].

For example, AuNPs functionalized by *N*-lauroyltyramine (NLTA) were prepared for Al(III) sensing. The presence of Al(III) induced the nanoparticles' aggregation with the consequent color change from pink to purple. The selectivity was tested by analyzing several other metal ions. Among these metal ions, the NLTA-AuNPs aggregation was induced only after the addition of Al(III). The detection limit reported is about 1.15 μM , and the dose/response curve is linear from 0 to 12 μM . The sensor was applied to Al(III) detection in-ground and sewage waters, giving good recovery [105].

As well-known, arsenic is a very toxic element responsible for several acute and chronic poisoning in humans. AuNPs based colorimetric sensors for As(III) are generally based on the strong binding affinity of the cation to sulfur-containing compounds. Based on this property, Kalluri et al. functionalized AuNPs with glutathione, dithiothreitol, and cysteine for obtaining colorimetric sensors for As(III). The detection limit of the sensors was 5 ppb, 20 ppb, and 25 ppb for dithiothreitol, glutathione, and cysteine-conjugated NPs, respectively. The lower detection limit obtained for AuNPs functionalized with

dithiothreitol was probably due to the As-S bond; conversely, in the other two sensors, the bonds As-O were expected due to the lack of free SH groups [107].

Besides metal ions, colorimetric sensors based on AuNP aggregation were also developed for some organic molecules. For example, simultaneous recognition of amino acids by 4-aminonicotinic acid-functionalized AuNPs was proposed [108]. The presence of arginine, histidine, methionine and tryptophan, induced the nanoparticle's aggregation through electrostatic interactions and hydrogen bonding.

Specific and sensitive DNA detection is crucial for clinical diagnostics (for example, diagnosing genetic diseases, biodefense and RNA profiling). Interesting studies proposed the design of thiolated oligonucleotide modified AuNPs sensors. These probes possess complementary structures that capture target DNA, resulting in the hybridization of DNA into a double helix, self-assembly of AuNPs and a consequent change in the solution color [109].

4.2. Colorimetric Sensors Based on AuNP Anti-Aggregation

Nowadays, sensing based on AuNP anti-aggregation strategies has also been of interest. In these devices, generally, a reagent first provokes the aggregation of AuNPs. Then the addition of an analyte with a high affinity to the aggregating reagent deactivates the nanoparticles' aggregation in a degree proportional to its concentration. In this way, the process can be used for the analyte determination [105].

For example, Chen et al. developed a colorimetric sensor for Hg(II) ions based on anti-aggregation of AuNPs functionalized with thiocyanuric acid. The assay is based on the high affinity of mercury ions towards thiols. In the presence of thiocyanuric acid, gold nanoparticles aggregate thanks to the interaction between the Au surface and the thiol group inducing a color variation from red to blue. After adding Hg(II), the thiocyanuric acid is removed from the nanoparticle surface since mercury ions are more active towards thiols than gold; consequently, the anti-aggregation of AuNPs occurred, and the solution color turned from blue to red. The practical application of the method was evaluated by applying it to trace Hg(II) determination in certified reference material and natural waters, obtaining good recovery. Thanks to these results, the method can also be useful for Hg(II) determination at low concentrations below 1 nM [110].

Another more recent example proposed by Huang et al. relates the development of a colorimetric sensor for methionine in serum and urine, based on the anti-aggregation of AuNPs in the presence of melamine. Citrate capped AuNPs can aggregate in the presence of melamine due to the ligand exchange between the negatively charged citrate ions and the positively charged amino groups of melamine, inducing a solution color change from wine red to blue. Nevertheless, in the presence of methionine, the gold nanoparticles are more disposed to interact with it through Au-S and Au-N bonds, inducing the nanoparticles' anti-aggregation. To evaluate the sensor's practicability, analyses of human serum and urine samples spiked with methionine were performed. Thanks to the good recovery obtained (from 95 to 105%), the method could be promising for methionine determination in biological fluids [111].

4.3. Colorimetric Sensors Based on AuNPs Etching

Analytes with high redox potential or acting as complexing ligands of noble metal ions can be detected by AuNPs etching. For example, a colorimetric Cu(II) sensor based on AuNPs etching was developed. Firstly, AuNPs (capped with citrate) were stabilized by hexadecyltrimethylammonium bromide (CTAB) in an ammonium buffer solution. In the presence of $S_2O_3^{2-}$ solution, the formation of the complex $Au(S_2O_3)_2^{3-}$ occurred, and consequently, the stabilized gold nanoparticles were partly dissolved, with a decrease of the SPR absorption. After the addition of Cu(II) the dissolving process accelerated, and the solution color of the solution disappeared rapidly. Figure 8 shows a scheme of the process.

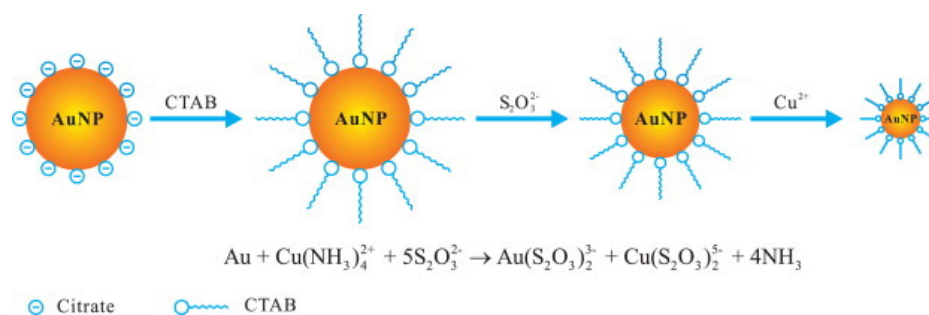


Figure 8. Scheme of the Cu(II) sensing based on the catalytic etching of AuNPs. Reprinted with permission from [112], copyright 2013 Elsevier B.V.

The color change induced by adding Cu^{2+} in concentration at least 40 nM can be easily observed by naked eyes so that the sensor can be promising for fast on-site analysis [112].

Based on the same principle, a cyanide sensor was proposed using gold nanorods (AuNRs). AuNRs were etched by cyanide at the transverse faces, leading to a variation of the AuNRs aspect (they were transformed from nanorods into nanosphere), resulting in a blue-shifted SPR absorption and color change from blue to pink [113].

4.4. Colorimetric Sensors Based on AuNP Anti-Etching

Some analytes can decrease or impede the etching of AuNPs, so the nanoparticles keep their initial morphology; this process can be useful to develop colorimetric sensors.

An interesting example was recently proposed by Wang et al. who developed a colorimetric sensor for sulfide ions using triangular Au nanoplates. In particular, the gold triangular nanoplates can be etched and transformed into nanospheres in the presence of triiodide ions produced by the reaction between Cu(II) and iodide. After adding sulfide ions, Cu(II) reacted preferentially with S^{2-} inhibiting the nanoplates etching; consequently, a redshift of the LSPR peak, proportional to the sulfide concentration, was observed. The sensor showed a linear response in the sulfide concentration range from 0.02 to 1.5 μM , with a LOD of about 16 nM. The good results obtained by applying the method to natural water samples make it promising for sulfide analyses of environmental matrices [114].

The same authors also proposed a colorimetric assay for the sequential determination of Cu(II) and Hg(II) still based on etching/anti-etching of gold nanoplates. Firstly Au nanoplates were etched in the presence of I_3^- obtained by a redox reaction between Cu(II) and an excess of iodide; the shape of the nanoplates changed from triangles to spheres, and a consequent color variation from blue to pink, of a degree proportional to Cu(II) concentration, can be observed. Then, after adding Hg(II) ions, the etching was inhibited since I^- was consumed for HgI_2 salt formation. Thus the nanoplates' shape has returned triangular, and the solution color varied from pink to blue, with an anti-etching degree proportional to Hg(II) concentration. The linearity of the dose-response curve was verified in the range 10 nM–1.5 μM for Cu(II) and 20 nM–3 μM for Hg(II). The LODs were reported equal to 19 nM and 9 nM, respectively, for Cu(II) and Hg(II). The method was applied for determining Cu(II) and Hg(II) in natural waters and food samples. Since the pretty good results, this colorimetric assay seems promising for a quick (the whole analysis has a duration of about 15 min) and sensible sequential determination of Cu(II) and Hg(II) [115].

4.5. Colorimetric Sensors Based on AuNP Growth

Some analytes with high reduction potential can react with AuCl_4^- to form nanoparticles so that when AuNPs act as seeds in the reaction between AuCl_4^- and a reductant, the formation of gold nanoshells on the surface of the nanoparticles induces a variation in the SPR spectrum. Gold nanoparticles, nanocages and nanorods were applied as seeds for the formation of nanoshells; during this process, the variation of the shape and composition of nanoparticles induces the change in the SPR spectrum and the consequent color change of

the solution. Sensors based on this phenomenon were developed to detect, for example, amino acids, *p*-aminophenol, catecholamine neurotransmitters and ellagic acid [116–119].

5. Ag/Au Bimetallic NPs

In the previous sections, we have described how Ag and Au NPs might be obtained and their respective applications, but we must stress that Ag/Au bimetallic NPs show different features and behaviors than monometallic ones. Bimetallic nanoparticles are often core shells, which means that the core and the shell are composed of two different metals, or Ag/Au alloys. The presence of two different metals in a single nanoparticle combined the performances of each one and had interesting catalytic activities; for example, the outer metal shell is electronically influenced by the metal inside the nucleus [120–122]. A very important feature of the bimetallic nanoparticles is that the SPR effect is emphasized compared to the monometallic ones [122].

Moreover, AgNPs have various disadvantages for their employment in sensors since their poor stability and less sensing reversibility due to light alteration, which makes their re-use less useful if compared with AuNPs. Improvements can be obtained by combining AgNPs with other metals, particularly gold, mainly forming Ag/Au core-shell structures or Ag/Au alloys [123].

Ag/Au core-shell NPs consist of two distinct layers, each made of one single metal. Generally, a gold shell and silver core were created to improve the stability of AgNPs; in this case, the synthesis involves electrodeposition of a thin film of gold on the silver core. Another method consists of laser ablation of gold in a colloidal solution of silver; in this way, an Ag core can be generated, and a gold layer grows on it [123].

Zhang et al. described a one-pot method for synthesizing PVP-protected-Ag core/Au shell nanoparticles with strong catalytic activity towards glucose oxidation. In order to form these NPs, to a water solution of $\text{AuCl}_4^-/\text{Ag}^+/\text{PVP}$, NaBH_4 is rapidly added as a reducing agent. With this method, a brown-colored colloidal solution is obtained. The nanoshells are filtered and washed with water and ethanol. The experiments were conducted with various ratios of Au and Ag, and the obtained colloidal solutions have different UV-Vis spectra. Furthermore, the results show that the core shells have higher catalytic activity for glucose oxidation than the enzyme [124].

The main synthesis of core-shell nanoparticles, with a silver shell on a gold core, is based on the reduction of silver nitrate at the gold-nanoparticles surface. The procedure needs a reducing agent, for example, citrate or ascorbate; thereby, the chemical deposition of silver on the gold core gives rise to spherical or rod-shaped structures.

Ag/Au alloy nanoparticles (AgAuNPs) are mixtures of atoms of both metals. The principal synthesis method of AgAuNPs is the co-reduction of silver nitrate and tetrachloroauric(III) acid with sodium citrate; in this case, small (about 20 nm) and spherical nanoparticles can be obtained. Ag/Au alloy nanoparticles can also be prepared by a physical method. For instance, the metal evaporation (evaporation of layers of silver and gold in a vacuum chamber) and the subsequent thermal treatment led to the formation of supported nanoparticles on glass. With this procedure, clusters of spherical (or quasi-spherical) AgAuNPs deposits on the glass support are obtained.

Ag/Au alloys nanoparticles are more stable than the core-shell ones of the same shape and size. Moreover, the proportion between the two metals in the alloy is an important factor to be taken into account for tuning the NPs absorption properties. Indeed, the SPR peak for spherical AgNPs is around 400 nm, and for AuNPs is about 520 nm; the SPR peak for the Ag/Au alloy nanoparticles will be tuned between the two values varying the alloy nanoparticles composition [123]. This section summarizes some recent applications of Ag/Au bimetallic NPs in colorimetric sensors, examining the different approaches based on nanoparticles' aggregation, etching or growth.

5.1. Colorimetric Sensors Based on Ag/Au Bimetallic NP Aggregation

Among the colorimetric sensors, those based on Ag/Au bimetallic NPs aggregation are the most developed. An interesting study proposed a colorimetric assay to detect Cd(II) in water samples using L-cysteine-functionalized Ag/Au nanoparticles. The sensor is based on the nanoparticles' aggregation induced by the interaction between Cd(II) and L-cysteine on the nanoparticles' surface, with a solution color change from yellow-orange to green. The Ag/Au bimetallic nanoparticles were synthesized by reducing silver nitrate and tetrachloroauric(III) acid in an aqueous solution, and they were subsequently functionalized with L-cysteine. The linearity of the response/dose graph was verified in the concentration range 0.4–38.6 μM Cd(II), and the LOD is about 44 nM. By interference study, the selectivity of the method was proved. The sensor was applied to the Cd(II) detection in real water samples. The results were in pretty good agreement with those obtained by the classical graphite furnace atomic absorption spectrometry (GFAAS) technique, verifying the good potential of the method for further applications in the environmental analysis [125].

Based on analogous principle, the same Zealandise research group developed a selective and simple colorimetric sensor for detecting the β -agonist ractopamine in animal, tissue, feed and urine samples. Ractopamine is a β -adrenergic agonist molecule that can improve fat catabolism when present in animal foods; nevertheless, it is banned in the EU, China and Thailand for the potential danger if humans ingest it, so it is fundamental to develop simple, selective and rapid methods for the accurate detection of ractopamine. In this matter, a colorimetric sensor could be a good option. The assay proposed here is based on the interaction between ractopamine and sulfanilic acid-modified Ag/Au alloy nanoparticles. The nanoparticles were prepared, as reported above, by reducing silver nitrate and tetrachloroauric(III) acid. Then they were functionalized with sulfanilic acid. The interaction between the sulfanilic acid on the nanoparticles' surface and ractopamine induced rapid aggregation with a consequent color change from yellow-orange to green. The proposed sensor was applied to ractopamine determination in pork, swine feed and urine samples showing good recoveries, and the results obtained were in good agreement with those achieved by HPLC. So the method could be promising for screening this analyte in food and other animal products [126].

A colorimetric sensor based on Ag/Au core-shell nanoparticles for palmatine detection in traditional Chinese drugs was recently developed. Palmatine is a protoberberine alkaloid found in several plants and applied as an anti-inflammatory and antibacterial agent in treating gastrointestinal and genitourinary disorders. The quantification of palmatine is thus fundamental in clinical and medical analysis. This work used bimetallic silver shell/ascorbate-capped, negatively charged gold nanoparticles for palmatine sensing; in particular, the best response was obtained with 5 nm Ag shell thickness. Moreover, the addition of sodium bisulfite significantly improves the nanoparticles' aggregation, increasing the method's sensitivity. The aggregation is due to the presence of positively charged protonated palmatine that induced the aggregation of the negative charge nanoparticles through electrostatic interaction and the corresponding color change from orange to green. The intensity of the color is linearly proportional to palmatine concentration from 0.096 μM to 0.288 μM . This rapid and selective sensor can be promising for palmatine detection in clinical samples [127].

Bi et al. developed a sensor for Hg(II) detection based on the colorimetric response induced by the aggregation of lysine-capped Au/Ag alloy nanocomposites. Lysine was used as a capping agent for the gold surface of the nanoparticles since it strongly interacts through the amino groups with Au. The addition of Hg(II) induced the aggregation of lysine-capped Au/Ag nanoparticles, with a degree proportional to the cation concentration and a related color change from yellow-orange to yellowish-green or gray. The response/dose curve is linear in the Hg(II) concentration range from 0.01 μM to 10.0 μM with a LOD of about 4.8 nM. This method shows good potential for routine Hg(II) screening in environmental samples [128].

Also for Hg(II) determination, a colorimetric sensor based on surface etching and aggregation effect of cysteine-modified Au/Ag core-shell nanorods was presented. The addition of Hg(II) at low levels (lower than 60 μM) induced the aggregation of colloidal Au-Ag core-shell nanorods for intense electrostatic interaction. Thus, the plasmonic absorption peak decreased rapidly, and color faded. Instead, if the Hg(II) addition were higher than 60 μM , the cysteine molecules came off from the nanorods' surface due to the intense interaction between the thiol group of the capping agent and Hg(II). Hence, the nanorods' etching occurred due to the decrease of the Ag shell, and the consequent color change from green to brown and then red was observed. From interference studies, good selectivity for Hg(II) was proved. The sensor was tested for tap water samples analysis, and the results agreed with the expected values; thus, the method could be considered suitable and reliable for Hg(II) determination in environmental samples [129].

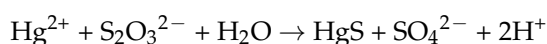
Recently, a colorimetric sensor for Mn(II) and ciprofloxacin detection was proposed based on bimetallic Ag-Au nanoparticles. An eco-friendly synthesis was used; indeed, the bimetallic nanoparticles were prepared by a β -cyclodextrin mediated microwave method. β -cyclodextrin acted as both a reducing and capping agent. The addition of Mn(II) to the Au/Ag nanoparticles' solution induced their aggregation and a consequent color change from brick red to rosy-brown, increasing Mn(II) concentration from 0.02 μM to 0.20 μM was observed. Also, adding ciprofloxacin to the same nanoparticles induced their aggregation, and a change in color of the solution from brick red to violet was observed by increasing the ciprofloxacin concentration. Since the good results were obtained by applying the method to Mn(II) determination in natural waters and ciprofloxacin in drugs, the sensor is promising for environmental and pharmaceutical analysis [130].

5.2. Colorimetric Sensors Based on Ag/Au Bimetallic NPs Etching

This section describes some colorimetric sensors based on the Ag/Au nanoobjects' morphology transformation, i.e., etching. A very recent study proposed a colorimetric device for detecting Cr(VI) in aqueous samples based on the etching of Au nano-double cone/Ag nanorods (Au-NDC@Ag-NRs) induced by the chromium(VI) ions. The sensing principle is here briefly explained. After adding HBr to the Au-NDC@Ag-NRs aqueous solution, bromide ions covered the nanoobjects' surface, making them unstable due to the strong acid media. The following addition of Cr(VI) to the solution promoted the dissolution of the silver shell and the gold core since the formation of silver and gold bromides and the size reduction of the nanoobjects occurred. As a consequence of the morphology transformation, a redshift of the absorption peak was observed. By increasing Cr(VI) concentration, the color changed from orange to pink, purple, and colorless at the highest detectable concentration (40 μM).

The linearity of the dose/response curve was in the range of 2.5–40 μM Cr(VI) concentration, and the LOD was about 1.7 μM . The good results obtained in the interference tests and the analysis of real water samples revealed excellent perspectives for practical applications [131].

Jinhua Wang et al. newly proposed a colorimetric sensor for Hg(II) based on the etching of Au/Ag nanoparticles. In this assay, adding an excess of thiosulfate to the nanoparticles' orange solution, the Ag shells were etched, and the solution changed its color to brick red. After the addition of Hg(II), the etching effect is suppressed proportionally to the metal-ion concentration since the following reaction happened:



The LOD of the method was 0.2 μM , and the linear range was from 0.2 to 10 μM . The applicability of the sensor was tested, determining Hg(II) in traditional Chinese drugs and real water samples; the results were promising for fast and on-site analysis [132].

Again, for detecting Hg(II), Chen et al. developed a sensor based on the etching of Au/Ag nanocages with a partial hollow cavity and several pinholes on the wall. The morphological transformation was induced by the reduction of Hg(II) to Hg(0) caused by

the Ag core of the nanocages. The mercury deposition on the inner surface of nanocages converted the hollow Au/Ag nanocages to closed nanoboxes with Au/Ag shell and Hg core with a consequent blue shift of the LSPR absorbance peak, proportional to the Hg(II) concentration. The sensor showed a linear response to Hg(II) concentration range from 0.03 to 35 μM and a LOD of 10 nM. Interference test and real lake and tap water samples analysis demonstrated the good potential for Hg(II) determination by the developed sensor [133].

As of the last examples, two interesting colorimetric sensors for glucose determination are described in the following paragraphs. He et al. described an optical sensor for glucose based on Ag/Au bimetallic nanoshells. The work aims to determine glucose concentration in solution monitoring the plasmonic band of Ag/Au nanoparticles. The sensing surface is composed of Ag/Au NPs with glucose oxidase (GOx) adsorbed onto the surface. In order to form the nanoparticles, AgNO_3 and citrate were used as starting materials, the obtained Ag colloidal solution was used as seeding solution, and NH_2OH and HAuClO_4 were added. In this way, citrate-stabilized Ag/Au NPs were obtained; they were functionalized with GOx through electrostatic adsorption. The detection mechanism of glucose in solution is based on the following reaction:



When this process occurs, the formed H_2O_2 reacts with Ag(0) of the NPs shell, forming Ag(I). The presence of monovalent Ag etched the nanoparticles and made them porous. This nanoparticles' change generated a redshift on the surface of the plasmon band, reflecting the concentration change of H_2O_2 , so by monitoring the red-shifted plasmon band of the nanoparticles, it was possible to determine the concentration of peroxide and so of glucose in solution [134].

In the second study, Ag/Au core/shell triangular nanoplates were applied. The glucose-sensing mechanism is based on the glucose oxidase-like activity of the Au shell that enabled the oxidation of glucose to produce hydrogen peroxide, which can further etch the silver core, leading to a nanoparticles' solution color change from blue to colorless. Compared with other NPs-based glucose devices, no enzymes or organic chromogenic agents were employed by this method; moreover, the Ag/Au core/shell triangular nanoplates are more stable than AgNPs since the Au shell protection. The method's applicability was proven by determining glucose in urine samples of patients with diabetes with a good % of recovery and results similar to those obtained with standard clinical analysis [135].

5.3. Colorimetric Sensors Based on Ag/Au Bimetallic NP Growth

Efforts on noble metal nanoparticles-based devices for sensing with a naked-eye readout confirm the advantages and the convenience of NPs growth-based analytical systems for use in biosensing, medical diagnosis, environmental protection and food safety monitoring. Good examples reported the utilization of different shell coatings on a seeding substrate, like the modulation of Ag shell growth on AuNPs substrate [136].

Guo et al. proposed a colorimetric sensor for determining biomolecules through enzyme-guided AgNPs growth on Au nanostars (AuNSs), using alkaline phosphatase (ALP) as a model analyte. The colorimetric detection of ALP was obtained in the presence of ascorbic acid 2-phosphate (AAP) and AuNSs, and it is due to the ALP-catalyzed dephosphorylation and the reduction of Ag^+ ions by ascorbic acid (AA) as shown in the scheme of Figure 9. The enzyme-guided growth of Ag nanoparticles on the gold nanostars induced the color change of the nanostars solution from blue to dark blue, purple and finally orange, proportionally to the ALP content.

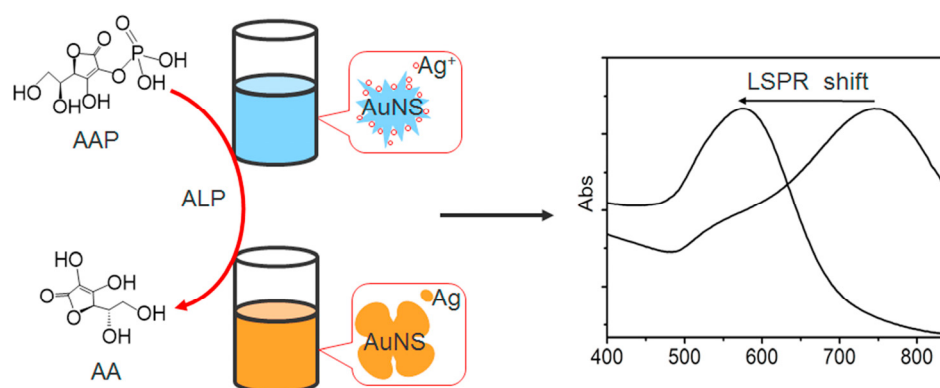


Figure 9. Scheme of the colorimetric sensor mechanism for ALP determination via enzyme-guided growth of AgNPs on AuNSs and the correspondent blue-shift of the LSPR peak. Reprinted with permission from [136], copyright 2015 Elsevier B.V.

By this method, a linear range from 1.0 pM to 25 nM and a LOD of 0.5 pM were reported. The proposed sensor could also be extended as a general device for detecting other biomolecules using ALP as a label, showing good perspectives for practical applications [136].

Lin et al. developed a colorimetric device for visual monitoring of food spoilage. It is based on the hydrolysis-induced Ag metallization of gold nanorods. Firstly, a sensory hydrogel was prepared by solidifying a mixture of gold nanorods, resorcinol monoacetate, and silver nitrate. Under the alkaline media, due to the presence of the biogenic amines, the hydrolysis of resorcinol monoacetate accelerated, producing resorcinol, which provoked the reduction of Ag(I) to Ag and the consequent deposition of silver shells on the gold nanorods. The growth of AgNPs on AuNRs is proportional to the pH and so to the amine concentration and consequently to the food spoilage degree. This process can be observed by naked eyes since the blue shift of the LSPR peak and the solution color change from pink to yellow, green, purple, and finally brick red by increasing the amine concentration. The applicability of the sensor was verified by applying the sensory hydrogels to monitor food spoilage in real samples such as fresh beef meat and salmon fish under different storage conditions. The color change of the hydrogels inside the packages, caused by volatile biogenic amines, provided visual information on the food's freshness [137].

6. Current Trends in Au and Ag Nanoparticle-Based Optical Devices

6.1. PAD Sensors

In recent years, it has become of increasing interest to develop low-cost, easy-to-use, environmentally friendly, portable sensors that require only a small quantity of sample for analysis [138]. One of the materials most suitable for these purposes is certainly paper. Obviously, there are many types of paper, but one readily available in a chemical laboratory is filter paper. Paper offers many advantages; besides being sustainable, it is easy to functionalize thanks to the presence of many hydroxyl groups on the surface of the molecule.

In 2020 Shariati and Khayatian have developed a paper-based analytical device (PAD), able to detect the presence of cysteine (Cys) and homocysteine (Hcy). The sensor is based on the interaction between Ag nanoparticles coated with 1,5-diphenylcarbazide (DPC) and the previously mentioned amino acids [139] (see Figure 10). As seen in the image below, a portion of filter paper is cut out to make a multi-way system for modification.

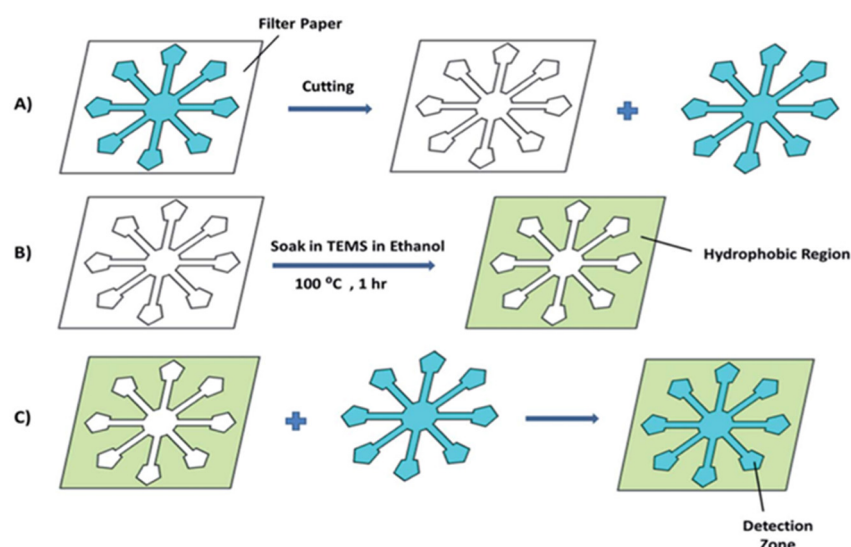


Figure 10. Surface modification of filter paper. (A) pattern design and cutting of the filter paper device, (B) Salinization of the hydrophilic filter paper device; (C) hydrophilic–hydrophobic contrast generated on the filter paper. Reprinted with permission from [139] under an Open-Access Creative Common CC license to RSC.

The star system will be the detection zone, while the part-colored green in the image is made hydrophobic so that it does not react with the samples but only acts as a support. Ag nanoparticles are synthesized from AgNO_3 reduced with NaBH_4 and then capped with DPC. To verify NPs interaction with Cys and Hcy, AgNPs were placed in contact with amino acids at different concentrations, studying the color formation and building up the related calibration curves. Once it was verified that the DPC-Ag NPs interacted with the two amino acids under investigation, the nanoparticle solution was deposited on the filter paper; then, increasing concentrations of both amino acids were deposited on each star tip (detection zone). By increasing the amino acid concentration, the intensity of the color on the filter paper tips increases from soft yellow (for a concentration of about $0.2 \mu\text{M}$) to intense pink (for a concentration of about $20 \mu\text{M}$).

The sensor was tested for other amino acids, but no evaluable color variation was registered. For this reason, the sensor's selectivity for Cys and Hcy was verified; in fact, the interaction of these two amino thiols with the donor groups of DPC induced the aggregation of nanoparticles and the consequent color variation. Since the amino acids examined are relevant in the human body, these sensors were applied to biological fluids such as urine. The good results obtained made the PAD promising for sensing Cys and Hcy in biological samples [139].

Other PAD sensors have been developed for metal ions determination. For example, in 2020 Shirvas et al. developed a sensor for detecting Fe(III) in environmental and biological samples [138]. The device consisted of filter paper impregnated with a solution of Ag-CTAB nanoparticles (silver nanoparticles capped with cetyltrimethylammonium bromide) able to interact with Fe(III) ions. The nanoparticles were prepared using NaBH_4 as a reductant and CTAB as a capping agent. Solutions with different concentrations of Fe(III) were put in contact with the sensing material, and it was noted that the nanoparticles began to change color from pronounced yellow to colorless by increasing the Fe(III) concentration. This effect is due to the electron transfer from CTAB to Fe(III). Once the color change is observed with the naked eye, images of the sensors were acquired with a smartphone and analyzed using the program ImageJ. This program can return the values of color intensity which will be used to build the calibration curve. The selectivity was confirmed by analyzing several metal cations, but the only effective response was obtained with Fe(III).

The same year, the Shirvas' research group developed an As(III) sensor based on a modified AuNPs sucrose capped PAD (AuNPs/Suc) [140]. Pink AuNPs solution was

obtained using HAuCl_4 as starting material, NaBH_4 as a reductant and Sucrose as a capping agent. After adding As(III) , the NPs solutions changed from pink to blue depending on the analyte concentration. The color variation was due to the nanoparticles' aggregation in the presence of As(III) , which causes the redshift of the LSPR band. Thanks to the positive response, the AuNPs/Suc was used as a printer ink to deposit dots of AuNPs/Suc on filter paper for producing a PAD sensor. After adding increasing As(III) concentrations, the dots changed colors from pink to intense blue, proportionally to the quantity of As(III) . Images of the sensor were collected using a smartphone, and the data obtained were processed for building the calibration curve.

The selectivity was tested by analyzing other cations such as Pb(II) , Tb(II) , Zn(II) , Fe(III) , Cd(II) , Y(II) , Cu(II) , La(III) , Hg(II) , Gd(III) , Na(I) , Ni(II) , K(I) , Ba(II) , but the positive response, due to AuNPs aggregation, was obtained only with As(III) .

The method's validity was proved by determining As(III) in real water (tube well, pond, river water) and soil samples; the results were not significantly different from those achieved with standard methods (ICP-OES), so the sensor demonstrated good potential for its application to environmental matrices.

Similarly to that for Fe(III) , a PAD sensor was developed for Hg(II) determination [141]. In this case, PVP-AgNPs were obtained by the reduction of AgNO_3 with NaBH_4 and using polyvinyl pyrrolidone (PVP) as a stabilizer. The PVP-AgNPs solution was placed in a printer cartridge and used as ink to print the sensor dots on a paper substrate. After adding Hg(II) to the sensor, the metal cation led to nanoparticles' disintegration and dissolution with a correspondent color change from yellow to colorless; indeed, the addition of Hg(II) caused the oxidation of Ag(0) to Ag(I) . Since several advantages of this PAD sensor, such as easy preparation, rapid response, low cost and disposable use, it can be efficiently applied to dose Hg(II) in environmental samples.

PADs were also be developed for anions determination; for example, Yakoh et al., in 2018, developed a sensor for chloride ions in environmental samples [142]. The nanospheres were obtained starting from AgNO_3 , NaBH_4 as reductant and starch as a stabilizer. The dark brown colloid indicates the formation of silver nanospheres. The colloid is boiled and then cooled down in order to remove NaBH_4 in excess. H_2O_2 is added to the system, and the colloid is stirred to ensure the completion of the reaction. Nanoprisms with different diameters were obtained, giving rise to different colored solutions. In order to obtain the best conditions, le nanoobjects with 35 nm and 45 nm diameters were chosen for their clearer color variation. In the first case, the presence of Cl^- turns the colloid from pink to yellow, in the second case from dark violet to red. The device was developed using the wax printing technique, where the wax was printed on paper to generate a pattern of hydrophobic barriers that did not interact with samples and colloids. Silver nanoprisms were absorbed onto the hydrophilic portion of the sensor, and standard solutions of Cl^- were added. The color change was visible to the naked eye after 3 min. The images were collected using a smartphone and analyzed with the ImageJ software to obtain the mean color intensity of every sensor's spot. The obtained values were plotted against $\log C$ (C is the Cl^- concentration) to calibrate the system.

By UV-vis spectroscopy, it was observed that the increase of Cl^- concentration provoked an oxidative etching of the silver nanoprisms with a consequent morphological transformation of the prisms from triangular or hexagonal to spherical. The change of the particles' shape caused a shift of the maximum LSPR peak and then a color change.

The method was successfully applied for determining Cl^- concentration in natural waters using the smartphone as a detector; since the results agreed to those obtained by standard methods, the sensor can be promising for in-lab and on-site determination of Cl^- in environmental samples.

Recently Zhang et al. developed a PAD for H_2O_2 determination in biological systems [143]. Carbon dots (CDs) were immobilized on a paper surface by covalent bonds. This structure shows a significant fluorescence signal. When deposited on the surface of the PCDs (paper functionalized with carbon dots), AgNPs acted as quenchers of fluorescence.

By contacting H_2O_2 with the AgNPs-PCDs, the nanoparticles were etched, so the fluorescence was restored. Unlike the previously described PAD sensors, this method required a more sophisticated apparatus for the analyses, but it needed low quantities of reagents and samples, and it can be easy to use and handle. The practical applicability of the method was evaluated by analyzing H_2O_2 in spiked milk samples. The good recovery revealed the potential of the sensor for detecting H_2O_2 in milk products. Moreover, the sensor showed good biocompatibility, so it could be applied for determining the hydrogen peroxide flux from living cells.

6.2. Biosensors

In recent years, the attention of researchers has been directed towards the use of biocompatible nanoparticles to constitute biosensors. Au NPs are among the most widely used materials because they are biocompatible, biodegradable and very stable [144]. An interesting feature of Au NPs is that the behavior of the nanoparticle under certain conditions is tunable or modifying the shape or functionalizing the surface with modifiers such as small molecules, polymers or macromolecules [145]. Au NPs based materials show outstanding enzyme-like characteristics; for example, they can mimic the behavior of peroxidase (POD) [146], oxidase (OXD) [147], superoxide dismutase (SOD) [148] and catalase (CAT) [149].

An emerging field in biosensing involves SPR sensors. They are widely used due to their rapid response, high sensitivity, high selectivity and low quantity of sample requirement. In 2021 Liu et al. developed an SPR sensor for the determination of RNA sequences. The study was performed using SARS-CoV-2 RNA sequences named RdRp as target molecule and AuNPs modified with SARS-CoV-2 DNA deposited on a selected surface as the sensing material. When the detection material is not in contact with the analyte (RdRp), the resonance angle θ assumes a certain value, but the resonance angle changes when the target is detected. The resonance angle shift $\Delta\theta$ is the recorded signal plotted against the RdRp concentration to obtain the calibration curve [150]. Aptamers are very specific; for this reason, these kinds of sensors are not very sensitive to the presence of interferents.

Huang et al. developed a sensor to detect miRNA (micro-RNA) using AuNPs to enhance the SPR signal [151]. The SPR chip surface was modified with streptavidin (SA), while DNA was modified with biotin (bio) at the beginning and the end of the filament (bio-DNA-bio). If the chip enters in contact only with bio-DNA-bio, one end of the filament interacts with the SA on the surface of the chip; the other end can interact with SA-AuNPs, which return a very intense SPR signal. The project aimed to detect miRNA. miRNA filament can interact selectively with the DNA filament. The authors decided to use duplex-specific nuclease (DSN), which is an enzyme able to cleave the DNA strand in double-stranded DNA or RNA/DNA hybrids. When the target miRNA in solution interacts with DNA, the formed hybrids are digested with DSN, and the obtained system contains undamaged miRNA and two pieces of DNA with only one biotin for each. The bio-DNA can react with the surface of the SPR chip but not with SA-AuNPs. Since the SA-AuNPs are not bound to the DNA, the sensor signal decreases proportionally to the miRNA concentration [151].

Another example of AuNPs used in SPR sensors is reported by Ferreira et al., who developed a biosensor to determine the cardiac biomarker creatine kinase (CK-MB). The gold substrate of the PCR chip is modified with 11-mercaptoundecanoic acid; thanks to this functionalization, the surface is negatively charged due to the exposure of the carboxyl groups (-COOH) than a cationic electrolyte (PEI) and an anionic electrolyte (PVS) were deposited. After the deposition of PVS, the surface is negatively charged due to the exposure of the $-SO_3^-$ group; this group can interact with AuNPs modified with cysteamine (Cys), positively charged at pH 7.4. Some pendants Cys molecules on the surface of AuNPs are used to secure the nanoparticle to the surface others are free and available to be bounded to the modified creatine phosphate (Pcrea). Pcrea is sensitive to the presence of the enzyme

CK-MB. Every deposition step was monitored by absorption kinetic in order to ensure that every step was completed correctly. Once the sensing material is ready, the measurements are carried out, observing the shift in resonance angle when the sensor detects the target (CK-MB) [152].

An interesting immunosensor for Igm was developed by Bereli et al. in 2021 based on the SPR signal. In this case, the Au surface was modified using 1,8-octanedithiol. The amine-functionalized nanoparticles were fixed to the surface thanks to the second thiol pendant of the 1,8-octanedithiol. Anti-Igm was fixed to the N of the AuNPs capping agent. The measurements were conducted monitoring the change in the refractive index while varying the concentration of the target Igm in solution [153].

A newly emerging field of SPR sensors provides the development of new devices using optical fiber. In these kinds of sensors, the detection part is assembled on a zone of an optical fiber deprived of the cladding. An example is the optical fiber sensor developed by Huong et al. in 2021 to determine bovine serum albumin (BSA). In this work, the optical fiber was deprived of the cladding and modified. In the first step, the clad-free fiber was silanized using APTES after forming hydroxyl groups (-OH) on the surface. After that, AuNPs were immobilized on the amine-modified sample. The modified fiber was then carboxy-functionalized using Mercaptosuccinic acid. The head of the modified optical fiber enters in contact with the sample thanks to a microfluidic system. When the BSA reaches the sensing zone, the refractive index (RI) changes. The intensity of transmitted light increases as the concentration of BSA in the solution increases [154].

In every example reported above, AuNPs are used to enhance the SPR signal and for their versatility since Au is biocompatible and can be contacted with biomolecules without ruining their structures and configurations.

7. Conclusions and Perspectives

In this paper, an overview of Ag and Au nanoparticles-based colorimetric sensors was presented. Metal nanoparticle-based colorimetric sensors are effective tools for determining several analytes in different samples thanks to the rapidity of the responses, the simple procedures and cost-effectiveness.

Recently pretty good results have been obtained by applying Ag and Au nanoparticles-based colorimetric sensors for the selective and sensitive recognition of various analytes such as inorganic species, pesticides, drugs, and biomolecules. In particular, the selectivity of these sensors can be tuned by functionalizing the nanoparticles with different organic and inorganic ligands.

Despite the rapid progress in developing metal nanoparticle-based colorimetric tools, their overall performance faces great challenges. A crucial point is preserving the chemical and optical stability of the Ag and AuNPs during their synthesis and functionalization. Moreover, these colorimetric assays are still mainly applied in research laboratories, so it is important to develop strategies for expanding their practical applications. For example, as the advances in analytical techniques and materials science improve the potential of plasmonic sensors, to significantly increase the applications of these tools, practical test strips can be prepared by immobilizing Ag and AuNPs on practical supports such as filter paper, plastic materials, agarose gel. Also, combining NPs with microfluidic paper-based devices should be a good strategy to reduce reagents, sample volumes, time of analysis. Colorimetric devices integrated with smartphone cameras could be developed for rapid clinical and environmental tests. Finally, a rational design of dual-mode sensors with both colorimetric and fluorometric readout should be developed. Given the above, the application of colorimetric sensors based on silver and gold nanomaterials in the chemical and biological fields is attractive and promising.

Author Contributions: Conceptualization, G.A., C.Z.; writing—original draft preparation, G.A., C.Z.; writing—review and editing G.A., C.Z., L.R.M., R.B. All authors have read and agreed to the published version of the manuscript.

Funding: This research received no external funding.

Institutional Review Board Statement: Not applicable.

Informed Consent Statement: Not applicable.

Data Availability Statement: Not applicable.

Conflicts of Interest: The authors declare no conflict of interest.

References

1. Wang, H.; Rao, H.; Luo, M.; Xue, X.; Xue, Z.; Lu, X. Noble metal nanoparticles growth-based colorimetric strategies: From monochrometric to multichrometric sensors. *Co-ord. Chem. Rev.* **2019**, *398*, 113003. [\[CrossRef\]](#)
2. Alberti, G.; Zaroni, C.; Magnaghi, L.R.; Biesuz, R. Disposable and Low-Cost Colorimetric Sensors for Environmental Analyses. *Int. J. Environ. Res. Public Health* **2020**, *17*, 8331. [\[CrossRef\]](#)
3. Zhang, Z.; Wang, H.; Chen, Z.; Wang, X.; Choo, J.; Chen, L. Plasmonic colorimetric sensors based on etching and growth of noble metal nanoparticles: Strategies and applications. *Biosens. Bioelectron.* **2018**, *114*, 52–65. [\[CrossRef\]](#) [\[PubMed\]](#)
4. Kangas, M.J.; Burks, R.; Atwater, J.; Lukowicz, R.M.; Williams, P.; Holmes, A.E. Colorimetric Sensor Arrays for the Detection and Identification of Chemical Weapons and Explosives. *Crit. Rev. Anal. Chem.* **2016**, *47*, 138–153. [\[CrossRef\]](#) [\[PubMed\]](#)
5. Pham, X.-H.; Hahm, E.; Kim, T.H.; Kim, H.-M.; Lee, S.H.; Lee, Y.-S.; Jeong, D.H.; Jun, B.-H. Enzyme-catalyzed Ag Growth on Au Nanoparticle-assembled Structure for Highly Sensitive Colorimetric Immunoassay. *Sci. Rep.* **2018**, *8*, 1–7. [\[CrossRef\]](#)
6. Shiping Song, D.L.; Fan, C. Target-Responsive Structural Switching for Nucleic Acid-Based Sensors. *Acc. Chem. Res.* **2010**, *43*, 631–641.
7. Lei, J.; Ju, H. Signal amplification using functional nanomaterials for biosensing. *Chem. Soc. Rev.* **2012**, *41*, 2122–2134. [\[CrossRef\]](#) [\[PubMed\]](#)
8. Lim, W.Q.; Gao, Z. Plasmonic nanoparticles in biomedicine. *Nano Today* **2016**, *11*, 168–188. [\[CrossRef\]](#)
9. Paterson, S.; de la Rica, R. Solution-based nanosensors for in-field detection with the naked eye. *Analyst* **2015**, *140*, 3308–3317. [\[CrossRef\]](#) [\[PubMed\]](#)
10. Ma, X.; He, S.; Qiu, B.; Luo, F.; Guo, L.; Lin, Z. Noble Metal Nanoparticle-Based Multicolor Immunoassays: An Approach toward Visual Quantification of the Analytes with the Naked Eye. *ACS Sens.* **2019**, *4*, 782–791. [\[CrossRef\]](#) [\[PubMed\]](#)
11. Ma, X.; Sun, H.; Wang, Y.; Wu, X.; Zhang, J. Electronic and optical properties of strained noble metals: Implications for applications based on LSPR. *Nano Energy* **2018**, *53*, 932–939. [\[CrossRef\]](#)
12. Saha, K.; Agasti, S.; Kim, C.; Li, X.; Rotello, V.M. Gold Nanoparticles in Chemical and Biological Sensing. *Chem. Rev.* **2012**, *112*, 2739–2779. [\[CrossRef\]](#) [\[PubMed\]](#)
13. Islam, M.N.; Yadav, S.; Haque, M.H.; Munaz, A.; Islam, F.; Al Hossain, M.S.; Gopalan, V.; Lam, A.K.; Nguyen, N.-T.; Shiddiky, M.J. Optical biosensing strategies for DNA methylation analysis. *Biosens. Bioelectron.* **2017**, *92*, 668–678. [\[CrossRef\]](#) [\[PubMed\]](#)
14. Mirkin, C.A.; Letsinger, R.L.; Mucic, R.C.; Storhoff, J.J. A DNA-based method for rationally assembling nanoparticles into macroscopic materials. *Nature* **1996**, *382*, 607–609. [\[CrossRef\]](#)
15. Citartan, M.; Tang, T.-H. Recent developments of aptasensors expedient for point-of-care (POC) diagnostics. *Talanta* **2019**, *199*, 556–566. [\[CrossRef\]](#)
16. Howes, P.; Rana, S.; Stevens, M.M. Plasmonic nanomaterials for biodiagnostics. *Chem. Soc. Rev.* **2013**, *43*, 3835–3853. [\[CrossRef\]](#) [\[PubMed\]](#)
17. Ajay, P.V.S.; Printo, J.; Kiruba, D.S.C.G.; Susithra, L.; Takatoshi, K.; Sivakumar, M. Colorimetric sensors for rapid detection of various analytes. *Mater. Sci. Eng.* **2017**, *78*, 1231–1245.
18. Cao, J.; Sun, T.; Grattan, K. Gold nanorod-based localized surface plasmon resonance biosensors: A review. *Sens. Actuators B Chem.* **2014**, *195*, 332–351. [\[CrossRef\]](#)
19. Li, Y.; Wang, Z.; Sun, L.; Liu, L.; Xu, C.; Kuang, H. Nanoparticle-based sensors for food contaminants. *TrAC Trends Anal. Chem.* **2019**, *113*, 74–83. [\[CrossRef\]](#)
20. Vert, M.; Doi, Y.; Hellwich, K.-H.; Hess, M.; Hodge, P.; Kubisa, P.; Rinaudo, M.; Schué, F. Terminology for biorelated polymers and applications (IUPAC Recommendations 2012). *Pure Appl. Chem.* **2012**, *84*, 377–410. [\[CrossRef\]](#)
21. Schaming, D.; Remita, H. Nanotechnology: From the ancient time to nowadays. *Found. Chem.* **2015**, *17*, 187–205. [\[CrossRef\]](#)
22. Khan, I.; Saeed, K.; Khan, I. Nanoparticles: Properties, applications and toxicities. *Arab. J. Chem.* **2019**, *12*, 908–931. [\[CrossRef\]](#)
23. Jamkhande, P.G.; Ghule, N.W.; Bamer, A.H.; Kalaskar, M.G. Metals nanoparticles synthesis: An overview on methods of preparation, advantages and disadvantages, and applications. *J. Drug. Deliv. Sci. Technol.* **2019**, *53*, 101174. [\[CrossRef\]](#)
24. Hartlieb, K.J.; Saunders, M.; Jachuck, R.J.J.; Raston, C. Continuous flow synthesis of small silver nanoparticles involving hydrogen as the reducing agent. *Green Chem.* **2010**, *12*, 1012–1017. [\[CrossRef\]](#)
25. Agunloye, E.; Panariello, L.; Gavriilidis, A.; Mazzei, L. A model for the formation of gold nanoparticles in the citrate synthesis method. *Chem. Eng. Sci.* **2018**, *191*, 318–331. [\[CrossRef\]](#)
26. Sun, K.; Qiu, J.; Liu, J.; Miao, Y. Preparation and characterization of gold nanoparticles using ascorbic acid as reducing agent in reverse micelles. *J. Mater. Sci.* **2009**, *44*, 754–758. [\[CrossRef\]](#)

27. Ahmed, K.B.A.; Kalla, D.; Uppuluri, K.B.; Anbazhagan, V. Green synthesis of silver and gold nanoparticles employing levan, a biopolymer from *Acetobacter xylinum* NCIM 2526, as a reducing agent and capping agent. *Carbohydr. Polym.* **2014**, *112*, 539–545. [[CrossRef](#)] [[PubMed](#)]
28. García-Barrasa, J.; López-De-Luzuriaga, J.M.; Monge, M. Silver nanoparticles: Synthesis through chemical methods in solution and biomedical applications. *Open Chem.* **2011**, *9*, 7–19. [[CrossRef](#)]
29. Verma, S.; Kumar, S.; Gokhale, R.; Burgess, D.J. Physical stability of nanosuspensions: Investigation of the role of stabilizers on Ostwald ripening. *Int. J. Pharm.* **2011**, *406*, 145–152. [[CrossRef](#)] [[PubMed](#)]
30. He, F.; Zhao, D. Manipulating the Size and Dispersibility of Zerovalent Iron Nanoparticles by Use of Carboxymethyl Cellulose Stabilizers. *Environ. Sci. Technol.* **2007**, *41*, 6216–6221. [[CrossRef](#)] [[PubMed](#)]
31. Casu, A.; Cabrini, E.; Donà, A.; Falqui, A.; Diaz-Fernandez, Y.; Milanese, C.; Taglietti, A.; Pallavicini, P. Controlled Synthesis of Gold Nanostars by Using a Zwitterionic Surfactant. *Chem.—A Eur. J.* **2012**, *18*, 9381–9390. [[CrossRef](#)] [[PubMed](#)]
32. Xie, J.; Lee, J.Y.; Wang, D.I.C.; Ting, Y.P. Silver Nanoplates: From Biological to Biomimetic Synthesis. *ACS Nano* **2007**, *1*, 429–439. [[CrossRef](#)] [[PubMed](#)]
33. Bronstein, L.M.; Shifrin, Z.B. Dendrimers as Encapsulating, Stabilizing, or Directing Agents for Inorganic Nanoparticles. *Chem. Rev.* **2011**, *111*, 5301–5344. [[CrossRef](#)] [[PubMed](#)]
34. Turkevich, J.; Stevenson, P.C.; Hillier, J. A study of the nucleation and growth processes in the synthesis of colloidal gold. *Discuss. Faraday Soc.* **1951**, *11*, 55–75. [[CrossRef](#)]
35. Preciado-Flores, S.; Wheeler, D.A.; Tran, T.M.; Tanaka, Z.; Jiang, C.; Barboza-Flores, M.; Qian, F.; Li, Y.; Chen, B.; Zhang, J.Z. SERS spectroscopy and SERS imaging of *Shewanella oneidensis* using silver nanoparticles and nanowires. *Chem. Commun.* **2011**, *47*, 4129–4131. [[CrossRef](#)] [[PubMed](#)]
36. Brust, M.; Walker, M.; Bethell, D.; Schiffrin, D.J.; Whyman, R. Synthesis of thiol-derivatised gold nanoparticles in a two-phase Liquid–Liquid system. *J. Chem. Soc. Chem. Commun.* **1994**, 801–802. [[CrossRef](#)]
37. Zhang, Q.; Hu, Y.; Guo, S.; Goebel, J.; Yin, Y. Seeded Growth of Uniform Ag Nanoplates with High Aspect Ratio and Widely Tunable Surface Plasmon Bands. *Nano Lett.* **2010**, *10*, 5037–5042. [[CrossRef](#)] [[PubMed](#)]
38. Bae, Y.; Kim, N.H.; Kim, M.; Lee, K.Y.; Han, S.W.H. Anisotropic Assembly of Ag Nanoprisms. *J. Am. Chem. Soc.* **2008**, *130*, 5432–5433. [[CrossRef](#)] [[PubMed](#)]
39. D’Agostino, A.; Giovannozzi, A.M.; Mandrile, L.; Sacco, A.; Rossi, A.M.; Taglietti, A. In situ seed-growth synthesis of silver nanoplates on glass for the detection of food contaminants by surface enhanced Raman scattering. *Talanta* **2020**, *216*, 120936. [[CrossRef](#)] [[PubMed](#)]
40. Rovati, D.; Albini, B.; Galinetto, P.; Grisoli, P.; Bassi, B.; Pallavicini, P.; Dacarro, G.; Taglietti, A. High Stability Thiol-Coated Gold Nanostars Monolayers with Photo-Thermal Antibacterial Activity and Wettability Control. *Nanomaterials* **2019**, *9*, 1288. [[CrossRef](#)] [[PubMed](#)]
41. Fernández-Lodeiro, A.; Djafari, J.; Fernández-Lodeiro, J.; Duarte, M.; Mauricio, E.M.; Capelo-Martínez, J.; Lodeiro, C. Synthesis of Mesoporous Silica Coated Gold Nanorods Loaded with Methylene Blue and Its Potentials in Antibacterial Applications. *Nanomaterials* **2021**, *11*, 1338. [[CrossRef](#)] [[PubMed](#)]
42. Naveenraj, S.; Mangalaraja, R.V.; Wu, J.J.; Asiri, A.M.; Anandan, S. Gold Triangular Nanoprisms and Nanodecahedra: Synthesis and Interaction Studies with Luminol toward Biosensor Applications. *Langmuir* **2016**, *32*, 11854–11860. [[CrossRef](#)]
43. Vigneshwaran, N.; Nachane, R.P.; Balasubramanya, R.H.; Varadarajan, P.V. A novel one-pot ‘green’ synthesis of stable silver nanoparticles using soluble starch. *Carbohydr. Res.* **2006**, *341*, 2012–2018. [[CrossRef](#)] [[PubMed](#)]
44. Nakhjavani, M.; Nikkhah, V.; Sarafraz, M.M.; Shoja, S. Green synthesis of silver nanoparticles using green tea leaves: Experimental study on the morphological, rheological and antibacterial behaviour. *Heat Mass Transf.* **2017**, *53*, 3201–3209. [[CrossRef](#)]
45. Daizy, P. Honey mediated green synthesis of gold nanoparticles. *Spectrom. Acta Part A* **2009**, *73*, 650–653.
46. Harlepp, S.; Robert, J.; Darnton, N.C.; Chatenay, D. Subnanometric measurements of evanescent wave penetration depth using total internal reflection microscopy combined with fluorescent correlation spectroscopy. *Appl. Phys. Lett.* **2004**, *85*, 3917. [[CrossRef](#)]
47. Cennamo, N.; Pesavento, M.; Zeni, L. A review on simple and highly sensitive plastic optical fiber probes for bio-chemical sensing. *Sens. Actuators B Chem.* **2020**, *331*, 129393. [[CrossRef](#)]
48. Cennamo, N.; Massarotti, D.; Conte, L.; Zeni, L. Low Cost Sensors Based on SPR in a Plastic Optical Fiber for Biosensor Implementation. *Sensors* **2011**, *11*, 11752–11760. [[CrossRef](#)]
49. Dwivedi, Y.S.; Sharma, A.K.; Gupta, B.D. Influence of Design Parameters on the Performance of a Surface Plasmon Sensor Based Fiber Optic Sensor. *Plasmonics* **2008**, *3*, 79–86. [[CrossRef](#)]
50. Rycenga, M.; Cobley, C.M.; Zeng, J.; Li, W.; Moran, C.H.; Zhang, Q.; Qin, D.; Xia, Y. Controlling the Synthesis and Assembly of Silver Nanostructures for Plasmonic Applications. *Chem. Rev.* **2011**, *111*, 3669–3712. [[CrossRef](#)] [[PubMed](#)]
51. Pastoriza-Santos, I.; Liz-Marzán, L.M. Colloidal silver nanoplates. State of the art and future challenges. *J. Mater. Chem.* **2008**, *18*, 1724–1737. [[CrossRef](#)]
52. Wiley, B.J.; Im, S.H.; Li, Z.-Y.; McLellan, J.; Siekkinen, A.A.; Xia, Y. Maneuvering the Surface Plasmon Resonance of Silver Nanostructures through Shape-Controlled Synthesis. *J. Phys. Chem. B* **2006**, *110*, 15666–15675. [[CrossRef](#)]
53. Kreibitz, U.; Vollmer, M. *Optical Properties of Metal Clusters*; Springer: New York, NY, USA, 1995.
54. Olson, J.; Dominguez-Medina, S.; Hoggard, A.; Wang, L.Y.; Chang, W.S.; Link, S. Optical Characterization of Single Plasmonic Nanoparticles. *Chem. Soc. Rev.* **2015**, *44*, 40–57. [[CrossRef](#)] [[PubMed](#)]

55. Amendola, V.; Meneghetti, M. Size Evaluation of Gold Nanoparticles by UV-vis Spectroscopy. *J. Phys. Chem. C* **2009**, *113*, 4277–4285. [[CrossRef](#)]
56. Jain, P.; Huang, X.; El-Sayed, I.H.; El-Sayed, M.A. Noble Metals on the Nanoscale: Optical and Photothermal Properties and Some Applications in Imaging, Sensing, Biology, and Medicine. *Accounts Chem. Res.* **2008**, *41*, 1578–1586. [[CrossRef](#)] [[PubMed](#)]
57. Khlebtsov, N.; Dykman, L. Biodistribution and toxicity of engineered gold nanoparticles: A review of in vitro and in vivo studies. *Chem. Soc. Rev.* **2011**, *40*, 1647–1671. [[CrossRef](#)] [[PubMed](#)]
58. Lee, S.H.; Jun, B.-H. Silver Nanoparticles: Synthesis and Application for Nanomedicine. *Int. J. Mol. Sci.* **2019**, *20*, 865. [[CrossRef](#)] [[PubMed](#)]
59. Beyene, H.D.; Werkneh, A.A.; Bezabh, H.K.; Ambaye, T.G. Synthesis paradigm and applications of silver nanoparticles (AgNPs), a review. *Sustain. Mater. Technol.* **2017**, *13*, 18–23. [[CrossRef](#)]
60. Yaqoob, A.A.; Umar, K.; Ibrahim, M.N.M. Silver nanoparticles: Various methods of synthesis, size affecting factors and their potential applications—A review. *Appl. Nanosci.* **2020**, *10*, 1369–1378. [[CrossRef](#)]
61. Gardea-Torresdey, J.L.; Gomez, E.; Peralta-Videa, J.R.; Parsons, J.G.; Troiani, A.H.; Jose-Yacaman, M. Alfalfa Sprouts: A Natural Source for the Synthesis of Silver Nanoparticles. *Langmuir* **2003**, *19*, 1357–1361. [[CrossRef](#)]
62. Ahmed, S.; Ahmad, M.; Swami, B.L.; Ikram, S. A review on plants extract mediated synthesis of silver nanoparticles for antimicrobial applications: A green expertise. *J. Adv. Res.* **2015**, *7*, 17–28. [[CrossRef](#)] [[PubMed](#)]
63. Mukherjee, P.; Ahmad, A.; Mandal, D.; Senapati, S.; Sainkar, S.R.; Khan, M.I.; Parishcha, R.; Ajaykumar, P.V.; Alam, M.; Kumar, R.; et al. Fungus-Mediated Synthesis of Silver Nanoparticles and Their Immobilization in the Mycelial Matrix: A Novel Biological Approach to Nanoparticle Synthesis. *Nano Lett.* **2001**, *1*, 515–519. [[CrossRef](#)]
64. Thakkar, K.N.; Mhatre, S.S.; Parikh, R.Y. Biological synthesis of metallic nanoparticles. *Nanomed. Nanotechnol. Biol. Med.* **2010**, *6*, 257–262. [[CrossRef](#)] [[PubMed](#)]
65. Elahi, N.; Kamali, M.; Baghersad, M.H. Recent biomedical applications of gold nanoparticles: A review. *Talanta* **2018**, *184*, 537–556. [[CrossRef](#)] [[PubMed](#)]
66. De Freitas, L.F.; Varca, G.H.C.; Batista, J.G.D.S.; Lugão, A.B. An Overview of the Synthesis of Gold Nanoparticles Using Radiation Technologies. *Nanomaterials* **2018**, *8*, 939. [[CrossRef](#)] [[PubMed](#)]
67. Sengani, M.; Grumezescu, A.M.; Rajeswari, V.D. Recent trends and methodologies in gold nanoparticle synthesis—A prospective review on drug delivery aspect. *OpenNano* **2017**, *2*, 37–46. [[CrossRef](#)]
68. Nune, S.K.; Chanda, N.; Shukla, R.; Katti, K.; Kulkarni, R.R.; Thilakavathi, S.; Mekapothula, S.; Kannan, R.; Katti, K.V. Green Nanotechnology from Tea: Phytochemicals in Tea as Building Blocks for Production of Biocompatible Gold Nanoparticles. *J. Mater. Chem.* **2009**, *19*, 2912–2920. [[CrossRef](#)] [[PubMed](#)]
69. Katti, K.K.; Chanda, N.; Shukla, R.; Zambre, A.; Suibramanian, T.; Kulkarni, R.R.; Kannan, R.; Katti, K.V. Green Nanotechnology from Cumin Phytochemicals: Generation of Biocompatible Gold Nanoparticles. *Int. J. Nanotechnol. Biomed.* **2009**, *1*, 39–52. [[CrossRef](#)]
70. Sharma, N.; Pinnaka, A.K.; Raje, M.; Fnu, A.; Bhattacharyya, M.S.; Choudhury, A.R. Exploitation of marine bacteria for production of gold nanoparticles. *Microb. Cell Factories* **2012**, *11*, 86. [[CrossRef](#)] [[PubMed](#)]
71. Mukherjee, P.; Senapati, S.; Mandal, D.; Ahmad, A.; Khan, M.I.; Kumar, R.; Sastry, M. Extracellular Synthesis of Gold Nanoparticles by the Fungus *Fusarium oxysporum*. *ChemBioChem* **2002**, *3*, 461–463. [[CrossRef](#)]
72. Vilela, D.; González, M.C.; Escarpa, A. Sensing colorimetric approaches based on gold and silver nanoparticles aggregation: Chemical creativity behind the assay. A review. *Anal. Chim. Acta* **2012**, *751*, 24–43. [[CrossRef](#)] [[PubMed](#)]
73. Roto, R.; Mellisani, B.; Kuncaka, A.; Mudasar, M.; Suratman, A. Colorimetric Sensing of Pb²⁺ Ion by Using Ag Nanoparticles in the Presence of Dithizone. *Chemosensors* **2019**, *7*, 28. [[CrossRef](#)]
74. Khan, N.A.; Niaz, A.; Zaman, M.I.; Khan, F.A.; Nisar-Ul-Haq, M.; Tariq, M. Sensitive and selective colorimetric detection of Pb²⁺ by silver nanoparticles synthesized from *Aconitum violaceum* plant leaf extract. *Mater. Res. Bull.* **2018**, *102*, 330–336. [[CrossRef](#)]
75. Shrivastava, K.; Sahu, B.; Deb, M.K.; Thakur, S.S.; Sahu, S.; Kurrey, R.; Kant, T.; Patle, T.K.; Jangde, R. Colorimetric and paper-based detection of lead using PVA capped silver nanoparticles: Experimental and theoretical approach. *Microchem. J.* **2019**, *150*. [[CrossRef](#)]
76. Ahmed, F.; Kabir, H.; Xiong, H. Dual Colorimetric Sensor for Hg²⁺/Pb²⁺ and an Efficient Catalyst Based on Silver Nanoparticles Mediating by the Root Extract of *Bistorta amplexicaulis*. *Front. Chem.* **2020**, *8*, 591958. [[CrossRef](#)] [[PubMed](#)]
77. Kumar, V.; Singh, D.K.; Mohan, S.; Bano, D.; Gundampati, R.K.; Hasan, S.H. Green synthesis of silver nanoparticle for the selective and sensitive colorimetric detection of mercury (II) ion. *J. Photochem. Photobiol. B Biol.* **2017**, *168*, 67–77. [[CrossRef](#)] [[PubMed](#)]
78. Dong, Y.; Ding, L.; Jin, X.; Zhu, N. Silver nanoparticles capped with chalcon carboxylic acid as a probe for colorimetric determination of cadmium(II). *Microchim. Acta* **2017**, *184*, 3357–3362. [[CrossRef](#)]
79. Almaquer, F.E.P.; Ricacho, J.S.Y.; Ronquillo, R.L.G. Simple and rapid colorimetric sensing of Ni(II) ions in tap water based on aggregation of citrate-stabilized silver nanoparticles. *Sustain. Environ. Res.* **2019**, *29*, 1–10. [[CrossRef](#)]
80. Sharma, R.; Dhillon, A.; Kumar, D. Mentha-Stabilized Silver Nanoparticles for High-Performance Colorimetric Detection of Al(III) in Aqueous Systems. *Sci. Rep.* **2018**, *8*, 5189. [[CrossRef](#)] [[PubMed](#)]
81. Sebastian, M.; Aravind, A.; Mathew, B. Green Silver Nanoparticles Based Multi-Technique Sensor for Environmental Hazardous Cu(II) Ion. *BioNanoScience* **2019**, *9*, 373–385. [[CrossRef](#)]

82. Chavada, V.D.; Bhatt, N.M.; Sanyal, M.; Shrivastav, P.S. Dual Fluorescence-colorimetric Silver Nanoparticles Based Sensor for Determination of Olanzapine: Analysis in Rat Plasma and Pharmaceuticals. *J. Fluoresc.* **2020**, *30*, 955–967. [[CrossRef](#)] [[PubMed](#)]
83. Shanmugaraj, K.; Sasikumar, T.; Campos, C.H.; Ilanchelian, M.; Mangalaraja, R.V.; Torres, C.C. Colorimetric determination of cysteamine based on the aggregation of polyvinylpyrrolidone-stabilized silver nanoparticles. *Spectrochim. Acta Part A Mol. Biomol. Spectrosc.* **2020**, *236*, 118281. [[CrossRef](#)]
84. Alula, M.T.; Karamchand, L.; Hendricks, N.R.; Blackburn, J.M. Citrate-capped silver nanoparticles as a probe for sensitive and selective colorimetric and spectrophotometric sensing of creatinine in human urine. *Anal. Chim. Acta* **2018**, *1007*, 40–49. [[CrossRef](#)]
85. Balasurya, S.; Syed, A.; Thomas, A.M.; Bahkali, A.H.; Elgorban, A.M.; Raju, L.L.; Khan, S.S. Highly sensitive and selective colorimetric detection of arginine by polyvinylpyrrolidone functionalized silver nanoparticles. *J. Mol. Liq.* **2019**, *300*, 112361. [[CrossRef](#)]
86. Yousefi, S.; Saraji, M. Optical aptasensor based on silver nanoparticles for the colorimetric detection of adenosine. *Spectrochim. Acta Part A Mol. Biomol. Spectrosc.* **2019**, *213*, 1–5. [[CrossRef](#)] [[PubMed](#)]
87. Zhai, X.; Li, Z.; Shi, J.; Huang, X.; Sun, Z.; Zhang, D.; Zou, X.; Sun, Y.; Zhang, J.; Holmes, M.; et al. A colorimetric hydrogen sulfide sensor based on gellan gum-silver nanoparticles bionanocomposite for monitoring of meat spoilage in intelligent packaging. *Food Chem.* **2019**, *290*, 135–143. [[CrossRef](#)] [[PubMed](#)]
88. Damalas, C.A.; Eleftherohorinos, I. Pesticide Exposure, Safety Issues, and Risk Assessment Indicators. *Int. J. Environ. Res. Public Heal.* **2011**, *8*, 1402–1419. [[CrossRef](#)] [[PubMed](#)]
89. Su, Y.-C.; Lin, A.-Y.; Hu, C.-C.; Chiu, T.-C. Functionalized silver nanoparticles as colorimetric probes for sensing triclyclazole. *Food Chem.* **2021**, *347*, 129044. [[CrossRef](#)] [[PubMed](#)]
90. Zheng, M.; Wang, C.; Wang, Y.; Wei, W.; Ma, S.; Sun, X.; He, J. Green synthesis of carbon dots functionalized silver nanoparticles for the colorimetric detection of phoxim. *Talanta* **2018**, *185*, 309–315. [[CrossRef](#)]
91. Ragam, P.N.; Mathew, B. Unmodified silver nanoparticles for dual detection of dithiocarbamate fungicide and rapid degradation of water pollutants. *Int. J. Environ. Sci. Technol.* **2019**, *17*, 1739–1752. [[CrossRef](#)]
92. Motahhari, A.; Abdolmohammad-Zadeh, H.; Farhadi, K. Development of a New Fluoride Colorimetric Sensor Based on Anti-aggregation of Modified Silver Nanoparticles. *Anal. Bioanal. Chem. Res.* **2021**, *8*, 79–89. [[CrossRef](#)]
93. Chavada, V.D.; Bhatt, N.M.; Sanyal, M.; Shrivastav, P.S. Pyrophosphate functionalized silver nanoparticles for colorimetric determination of deferiprone via competitive binding to Fe(III). *Microchim. Acta* **2017**, *184*, 4203–4208. [[CrossRef](#)]
94. Zheng, L.; Qi, P.; Zhang, D. A simple, rapid and cost-effective colorimetric assay based on the 4-mercaptophenylboronic acid functionalized silver nanoparticles for bacteria monitoring. *Sens. Actuators B Chem.* **2018**, *260*, 983–989. [[CrossRef](#)]
95. Mulvihill, M.; Ling, X.Y.; Henzie, J.; Yang, P. Anisotropic Etching of Silver Nanoparticles for Plasmonic Structures Capable of Single-Particle SERS. *J. Am. Chem. Soc.* **2009**, *132*, 268–274. [[CrossRef](#)]
96. Li, L.; Wang, J.; Chen, Z. Colorimetric determination of uric acid based on the suppression of oxidative etching of silver nanoparticles by chloroauric acid. *Microchim. Acta* **2019**, *187*, 18. [[CrossRef](#)] [[PubMed](#)]
97. Zhang, P.; Wang, L.; Zeng, J.; Tan, J.; Long, Y.; Wang, Y. Colorimetric captopril assay based on oxidative etching-directed morphology control of silver nanoprisms. *Microchim. Acta* **2020**, *187*, 107. [[CrossRef](#)] [[PubMed](#)]
98. Yuan, M.; Xiong, Q.; Zhang, G.; Xiong, Z.; Liu, D.; Duan, H.; Lai, W. Silver nanoprism-based plasmonic ELISA for sensitive detection of fluoroquinolones. *J. Mater. Chem. B* **2020**, *8*, 3667–3675. [[CrossRef](#)]
99. Tran, H.V.; Nguyen, T.V.; Nguyen, L.T.; Hoang, H.S.; Huynh, C.D. Silver nanoparticles as a bifunctional probe for label-free and reagentless colorimetric hydrogen peroxide chemosensor and cholesterol biosensor. *J. Sci. Adv. Mater. Devices* **2020**, *5*. [[CrossRef](#)]
100. Fang, X.; Ren, H.; Zhao, H.; Li, Z. Ultrasensitive visual and colorimetric determination of dopamine based on the prevention of etching of silver nanoprisms by chloride. *Microchim. Acta* **2016**, *184*, 415–421. [[CrossRef](#)]
101. Li, L.; Zhang, L.; Zhao, Y.; Chen, Z. Colorimetric detection of Hg(II) by measurement the color alterations from the “before” and “after” RGB images of etched triangular silver nanoplates. *Microchim. Acta* **2018**, *185*, 235. [[CrossRef](#)] [[PubMed](#)]
102. Li, P.; Lee, S.M.; Kim, H.Y.; Kim, S.; Park, S.; Park, K.S.; Park, H.G. Colorimetric detection of individual biothiols by tailor made reactions with silver nanoprisms. *Sci. Rep.* **2021**, *11*, 1–8. [[CrossRef](#)]
103. Afsharipour, R.; Shabani, A.M.H.; Dadfarnia, S.; Kazemi, E. Selective fluorometric determination of sulfadiazine based on the growth of silver nanoparticles on graphene quantum dots. *Microchim. Acta* **2019**, *187*, 1–8. [[CrossRef](#)] [[PubMed](#)]
104. Shaban, S.M.; Moon, B.-S.; Kim, D.-H. Selective and sensitive colorimetric detection of p-aminophenol in human urine and paracetamol drugs based on seed-mediated growth of silver nanoparticles. *Environ. Technol. Innov.* **2021**, *22*, 101517. [[CrossRef](#)]
105. Megarajan, S.; Veerappan, A. A selective pink-to-purple colorimetric sensor for aluminium via the aggregation of gold nanoparticles. *Opt. Mater.* **2020**, *108*, 110177. [[CrossRef](#)]
106. Yu, L.; Song, Z.; Peng, J.; Yang, M.; Zhi, H.; He, H. Progress of gold nanomaterials for colorimetric sensing based on different strategies. *TrAC Trends Anal. Chem.* **2020**, *127*, 115880. [[CrossRef](#)]
107. Kalluri, J.R.; Arbnesi, T.; Afrin Khan, S.; Neely, A.; Candice, P.; Varisli, B.; Washington, M.; McAfee, S.; Robinson, B.; Banerjee, S.; et al. Use of gold nanoparticles in a simple colorimetric and ultrasensitivedynamic light scattering assay: Selective detection of arsenic in groundwater. *Angew. Chem. Int. Ed.* **2009**, *48*, 1–5. [[CrossRef](#)]
108. Rawat, K.A.; Kailasa, S.K. 4-Amino nicotinic acid mediated synthesis of gold nanoparticles for visual detection of arginine, histidine, methionine and tryptophan. *Sens. Actuators B Chem.* **2016**, *222*, 780–789. [[CrossRef](#)]

109. Song, J.; Li, Z.; Cheng, Y.; Liu, C. Self-aggregation of oligonucleotide-functionalized gold nanoparticles and its applications for highly sensitive detection of DNA. *Chem. Commun.* **2010**, *46*, 5548–5550. [[CrossRef](#)]
110. Chen, Z.; Zhang, C.; Ma, H.; Zhou, T.; Jiang, B.; Chen, M.; Chen, X. A non-aggregation spectrometric determination for mercury ions based on gold nanoparticles and thiocyanuric acid. *Talanta* **2015**, *134*, 603–606. [[CrossRef](#)] [[PubMed](#)]
111. Huang, P.-C.; Gao, N.; Li, J.-F.; Wu, F.-Y. Colorimetric detection of methionine based on anti-aggregation of gold nanoparticles in the presence of melamine. *Sens. Actuators B Chem.* **2018**, *255*, 2779–2784. [[CrossRef](#)]
112. Liu, R.; Chen, Z.; Wang, S.; Qu, C.; Chen, L.; Wang, Z. Colorimetric sensing of copper(II) based on catalytic etching of gold nanoparticles. *Talanta* **2013**, *112*, 37–42. [[CrossRef](#)] [[PubMed](#)]
113. Lee, S.; Nam, Y.-S.; Choi, S.-H.; Lee, Y.; Lee, K.-B. Highly sensitive photometric determination of cyanide based on selective etching of gold nanorods. *Microchim. Acta* **2016**, *183*, 3035–3041. [[CrossRef](#)]
114. Wang, Q.; Wang, Y.; Guan, M.; Zhu, S.; Yan, X.; Lei, Y.; Shen, X.; Luo, L.; He, H. A multicolor colorimetric assay for sensitive detection of sulfide ions based on anti-etching of triangular gold nanoplates. *Microchem. J.* **2020**, *159*, 105429. [[CrossRef](#)]
115. Wang, Q.; Peng, R.; Wang, Y.; Zhu, S.; Yan, X.; Lei, Y.; Sun, Y.; He, H.; Luo, L. Sequential colorimetric sensing of cupric and mercuric ions by regulating the etching process of triangular gold nanoplates. *Microchim. Acta* **2020**, *187*, 205–209. [[CrossRef](#)] [[PubMed](#)]
116. Lin, T.; Li, Z.; Song, Z.; Chen, H.; Guo, L.; Fu, F.; Wu, Z. Visual and colorimetric detection of p-aminophenol in environmental water and human urine samples based on anisotropic growth of Ag nanoshells on Au nanorods. *Talanta* **2016**, *148*, 62–68. [[CrossRef](#)] [[PubMed](#)]
117. Wang, Y.; Zhang, P.; Mao, X.; Fu, W.; Liu, C. Seed-mediated growth of bimetallic nanoparticles as an effective strategy for sensitive detection of vitamin C. *Sens. Actuators B Chem.* **2016**, *231*, 95–101. [[CrossRef](#)]
118. Jafarinejad, S.; Ghazi-Khansari, M.; Ghasemi, F.; Sasanpour, P.; Hormozi-Nezhad, M.R. Colorimetric Fingerprints of Gold Nanorods for Discriminating Catecholamine Neurotransmitters in Urine Samples. *Sci. Rep.* **2017**, *7*, 1–8. [[CrossRef](#)]
119. Wang, Y.; Zeng, Y.; Fu, W.; Zhang, P.; Li, L.; Ye, C.; Yu, L.; Zhu, X.; Zhao, S. Seed-mediated growth of Au@Ag core-shell nanorods for the detection of ellagic acid in whitening cosmetics. *Anal. Chim. Acta* **2018**, *1002*, 97–104. [[CrossRef](#)] [[PubMed](#)]
120. Li, W.; Kuai, L.; Qin, Q.; Geng, B. Ag–Au bimetallic nanostructures: Co-reduction synthesis and their component-dependent performance for enzyme-free H₂O₂ sensing. *J. Mater. Chem. A* **2013**, *1*, 7111–7117. [[CrossRef](#)]
121. Tokonami, S.; Morita, N.; Takasaki, K.; Toshima, N. Novel Synthesis, Structure, and Oxidation Catalysis of Ag/Au Bimetallic Nanoparticles. *J. Phys. Chem. C* **2010**, *114*, 10336–10341. [[CrossRef](#)]
122. Huang, H.; Li, H.; Feng, J.-J.; Wang, A.-J. One-step green synthesis of fluorescent bimetallic Au/Ag nanoclusters for temperature sensing and in vitro detection of Fe³⁺. *Sens. Actuators B Chem.* **2015**, *223*, 550–556. [[CrossRef](#)]
123. Loiseau, A.; Asila, V.; Boitel-Aullen, G.; Lam, M.; Salmain, M.; Boujday, S. Silver-Based Plasmonic Nanoparticles for and Their Use in Biosensing. *Biosensors* **2019**, *9*, 78. [[CrossRef](#)] [[PubMed](#)]
124. Zhang, H.; Okuni, J.; Toshima, N. One-pot synthesis of Ag–Au bimetallic nanoparticles with Au shell and their high catalytic activity for aerobic glucose oxidation. *J. Colloid Interface Sci.* **2011**, *354*, 131–138. [[CrossRef](#)]
125. Du, J.; Hu, X.; Zhang, G.; Wu, X.; Gong, D. Colorimetric detection of cadmium in water using L-cysteine Functionalized gold–silver nanoparticles. *Anal. Lett.* **2018**, *51*, 2906–2919. [[CrossRef](#)]
126. Hu, X.; Du, J.; Pan, J.; Wang, F.; Gong, D. Zhang, G. Colorimetric detection of the β-agonist ractopamine in animal feed, tissue and urine samples using gold–silver alloy nanoparticles modified with sulfanilic acid. *Food Addit. Contam. Part. A* **2019**, *36*, 35–45. [[CrossRef](#)] [[PubMed](#)]
127. Gao, Y.; Hu, Z.; Wu, J.; Ning, Z.; Jian, J.; Zhao, T.; Liang, X.; Yang, X.; Yang, Z.; Zhao, Q.; et al. Size-tunable Au@Ag nanoparticles for colorimetric and SERS dual-mode sensing of palmitine in traditional Chinese medicine. *J. Pharm. Biomed. Anal.* **2019**, *174*, 123–133. [[CrossRef](#)] [[PubMed](#)]
128. Bi, N.; Zhang, Y.; Xi, Y.; Hu, M.; Song, W.; Xu, J.; Jia, L. Colorimetric response of lysine-capped gold/silver alloy nanocomposites for mercury(II) ion detection. *Colloids Surf. B Biointerfaces* **2021**, *205*, 111846. [[CrossRef](#)]
129. Zhu, J.; Zhao, B.-Z.; Qi, Y.; Li, J.-J.; Li, X.; Zhao, J.-W. Colorimetric determination of Hg(II) by combining the etching and aggregation effect of cysteine-modified Au-Ag core-shell nanorods. *Sens. Actuators B Chem.* **2018**, *255*, 2927–2935. [[CrossRef](#)]
130. George, J.M.; Priyanka, R.N.; Mathew, B. Bimetallic Ag–Au nanoparticles as pH dependent dual sensing probe for Mn(II) ion and ciprofloxacin. *Microchem. J.* **2020**, *155*, 104686. [[CrossRef](#)]
131. Liu, S.; Wang, X.; Zoua, C.; Zhouab, J.; Yanga, M.; Zhangab, S.; Huoa, D.; Houac, C. Colorimetric detection of Cr⁶⁺ ions based on surface plasma resonance using the catalytic etching of gold nano-double cone @ silver nanorods. *Anal. Chim. Acta* **2020**, *1149*, 238141. [[CrossRef](#)]
132. Wang, J.; Wu, J.; Zhang, Y.; Zhou, X.; Hu, Z.; Liao, X.; Sheng, B.; Yuan, K.; Wu, X.; Cai, H.; et al. Colorimetric and SERS dual-mode sensing of mercury (II) based on controllable etching of Au@Ag core/shell nanoparticles. *Sens. Actuators B Chem.* **2020**, *330*, 129364. [[CrossRef](#)]
133. Chen, J.-K.; Zhao, S.-M.; Zhu, J.; Li, J.-J.; Zhao, J.-W. Colorimetric determination and recycling of Hg²⁺ based on etching-induced morphology transformation from hollow AuAg nanocages to nanoboxes. *J. Alloys Compd.* **2020**, *828*, 154392. [[CrossRef](#)]
134. He, H.; Xu, X.; Wu, H.; Jin, Y. Enzymatic Plasmonic Engineering of Ag/Au Bimetallic Nanoshells and Their Use for Sensitive Optical Glucose Sensing. *Adv. Mater.* **2012**, *24*, 1736–1740. [[CrossRef](#)]

135. Liu, A.; Li, M.; Wang, J.; Feng, F.; Zhang, Y.; Qiu, Z.; Chen, Y.; Meteku, B.E.; Wen, C.; Yan, Z.; et al. Ag@Au core/shell triangular nanoplates with dual enzyme-like properties for the colorimetric sensing of glucose. *Chin. Chem. Lett.* **2020**, *31*, 1133–1136. [[CrossRef](#)]
136. Guo, Y.; Wu, J.; Li, J.; Ju, H. A plasmonic colorimetric strategy for biosensing through enzyme guided growth of silver nanoparticles on gold nanostars. *Biosens. Bioelectron.* **2015**, *78*, 267–273. [[CrossRef](#)]
137. Lin, T.; Wu, Y.; Li, Z.; Song, Z.; Guo, L.; Fu, F. Visual Monitoring of Food Spoilage Based on Hydrolysis-Induced Silver Metallization of Au Nanorods. *Anal. Chem.* **2016**, *88*, 11022–11027. [[CrossRef](#)] [[PubMed](#)]
138. Shrivasa, K.; Monisha; Kant, T.; Karbhal, I.; Kurrey, R.; Sahu, B.; Sinha, D.; Patra, G.K.; Deb, M.K.; Pervez, S. Smartphone coupled with paper-based chemical sensor for on-site determination of iron(III) in environmental and biological samples. *Anal. Bioanal. Chem.* **2020**, *412*, 1573–1583. [[CrossRef](#)] [[PubMed](#)]
139. Shariati, S.; Khayatian, G. The colorimetric and microfluidic paper-based detection of cysteine and homocysteine using 1,5-diphenylcarbazide-capped silver nanoparticles. *RSC Adv.* **2021**, *11*, 3295–3303. [[CrossRef](#)]
140. Shrivasa, K.; Patel, S.; Sinha, D.; Thakur, S.S.; Patle, T.K.; Kant, T.; Dewangan, K.; Satnami, M.L.; Nirmalkar, J.; Kumar, S. Colorimetric and smartphone-integrated paper device for on-site determination of arsenic (III) using sucrose modified gold nanoparticles as a nanoprobe. *Microchim. Acta* **2020**, *187*, 1–9. [[CrossRef](#)] [[PubMed](#)]
141. Monisha; Shrivasa, K.; Kant, T.; Patel, S.; Devi, R.; Dahariya, N.S.; Pervez, S.; Deb, M.K.; Rai, M.K.; Rai, J. Inkjet-printed paper-based colorimetric sensor coupled with smartphone for determination of mercury (Hg^{2+}). *J. Hazard. Mater.* **2021**, *414*, 125440. [[CrossRef](#)] [[PubMed](#)]
142. Yakoh, A.; Rattanarat, P.; Siangproh, W.; Chailapakul, O. Simple and selective paper-based colorimetric sensor for determination of chloride ion in environmental samples using label-free silver nanoprisms. *Talanta* **2018**, *178*, 134–140. [[CrossRef](#)] [[PubMed](#)]
143. Zhang, X.; Chen, S.; Zhuo, S.; Ji, Y.; Li, R. A carbon dots functionalized paper coupled with AgNPs composites platform: Application as a sensor for hydrogen peroxide detection based on surface plasmon-enhanced energy transfer. *New J. Chem.* **2021**. [[CrossRef](#)]
144. Liu, L.; Jiang, H.; Wang, X. Functionalized gold nanomaterials as biomimetic nanozymes and biosensing actuators. *TrAC Trends Anal. Chem.* **2021**, *143*, 116376. [[CrossRef](#)]
145. Biju, V. Chemical modifications and bioconjugate reactions of nanomaterials for sensing, imaging, drug delivery and therapy. *Chem. Soc. Rev.* **2013**, *43*, 744–764. [[CrossRef](#)] [[PubMed](#)]
146. Ni, P.; Dai, H.; Wang, Y.; Sun, Y.; Shi, Y.; Hu, J.; Li, Z. Visual detection of melamine based on the peroxidase-like activity enhancement of bare gold nanoparticles. *Biosens. Bioelectron.* **2014**, *60*, 286–291. [[CrossRef](#)] [[PubMed](#)]
147. Cao, G.-X.; Wu, X.-M.; Dong, Y.-M.; Li, Z.-J.; Wang, G.-L. Colorimetric determination of melamine based on the reversal of the mercury(II) induced inhibition of the light-triggered oxidase-like activity of gold nanoclusters. *Microchim. Acta* **2015**, *183*, 441–448. [[CrossRef](#)]
148. He, W.; Zhou, Y.-T.; Wamer, W.G.; Hu, X.; Wu, X.; Zheng, Z.; Boudreau, M.D.; Yin, J.-J. Intrinsic catalytic activity of Au nanoparticles with respect to hydrogen peroxide decomposition and superoxide scavenging. *Biomaterials* **2012**, *34*, 765–773. [[CrossRef](#)] [[PubMed](#)]
149. Lien, C.-W.; Chen, Y.-C.; Chang, H.-T.; Huang, C.-C. Logical regulation of the enzyme-like activity of gold nanoparticles by using heavy metal ions. *Nanoscale* **2013**, *5*, 8227–8234. [[CrossRef](#)] [[PubMed](#)]
150. Liu, L.; Ye, K.; Jia, Z.; Xue, T.; Nie, A.; Xiang, J.; Mu, C.; Wang, B.; Wen, F.; Zhai, K.; et al. High-sensitivity and versatile plasmonic biosensor based on grain boundaries in polycrystalline 1L WS₂ films. *Biosens. Bioelectron.* **2021**, *194*, 113596. [[CrossRef](#)] [[PubMed](#)]
151. Huang, Y.; Sun, T.; Liu, L.; Xia, N.; Zhao, Y.; Yi, X. Surface plasmon resonance biosensor for the detection of miRNAs by combining the advantages of homogeneous reaction and heterogeneous detection. *Talanta* **2021**, *234*, 122622. [[CrossRef](#)] [[PubMed](#)]
152. Ferreira, A.L.; de Lima, L.F.; Moraes, A.S.; Rubira, R.J.; Constantino, C.J.; Leite, F.L.; Delgado-Silva, A.O.; Ferreira, M. Development of a novel biosensor for Creatine Kinase (CK-MB) using Surface Plasmon Resonance (SPR). *Appl. Surf. Sci.* **2021**, *554*, 149565. [[CrossRef](#)]
153. Bereli, N.; Bakhshpour, M.; Topçu, A.A.; Denizli, A. Surface Plasmon Resonance-Based Immunosensor for Igm Detection with Gold Nanoparticles. *Micromachines* **2021**, *12*, 1092. [[CrossRef](#)] [[PubMed](#)]
154. Huong, V.T.; Phuong, N.T.T.; Tai, N.T.; An, N.T.; Lam, V.D.; Manh, D.H.; Chi, T.T.K.; Mai, N.X.D.; Phung, V.-D.; Tran, N.H.T. Gold Nanoparticles Modified a Multimode Clad-Free Fiber for Ultrasensitive Detection of Bovine Serum Albumin. *J. Nanomater.* **2021**, *2021*, 1–6. [[CrossRef](#)]